Plant Growth Regulation (2023) 101:743–767
https://doi.org/10.1007/s10725-023-01054-5

ORIGINAL PAPER

Silicon improves the growth of *Glycyrrhiza uralensis* Fisch. under salt and/or drought stress by regulating respiration metabolism

Ming Fan[1,4] · Enhe Zhang[1] · Xinhui Zhang[2,3] · Qinglin Liu[4] · Fengxia Guo[1,4]

Received: 19 February 2023 / Accepted: 21 July 2023 / Published online: 7 September 2023
© The Author(s) 2023

Abstract

Drought and salt stress severely threaten the growth and productivity of *Glycyrrhiza uralensis* Fisch. (*G.uralensis*), and usually, they occur concomitantly. Silicon (Si) addition is well known to enhance the tolerance of plants. Here, we analyzed the changes in parameters related to growth and respiration, including glycolysis pathway (EMP), tricarboxylic acid (TCA) cycle, and pentose phosphate pathway (PPP) by Si in *G. uralensis* seedlings under salt and/or drought stresses. Results showed that Si effectively alleviated the effect of salt, drought and combined stress on the growth and respiration metabolism of *G. uralensis* seedlings. Under salt stress, Si increased leaf number by 15.13%, upregulated the TCA pathway at the transcriptional level, and increased PFK, PK, and content of acetyl CoA in both aerial and underground, ICDHm, α-KGDH in aerial part and NAD-MDH in underground part, thus alleviating the inhibitory effect of salt stress on the EMP–TCA process, but weakening the PPP by declining G6PDH and 6-PGDH in aerial part by 34.10% and 55.54%, and G6PDH in underground part by 83.86%. Under drought stress, Si increased underground biomass by 11.40%, slowed the EMP by decreasing PFK in aerial part by 21.76%, PK and PFK in underground part by 38.11% and 64.71%, weakened PPP by reducing 6-PGDH in aerial part by 72.9%, G6PDH and 6-PGDH in underground part by 77.00% and 64.71%. Si increased SDH and phosphoenolpyruvate carboxylase (PEPC) by 28.66% and 145.48% with the TCA cycle and GABA shunt as the main respiratory pathways in the underground part of drought-stressed seedlings. Under combined stresses, Si addition increased leaf number and aboveground biomass by 11.96% and 23.88%, upregulated the EMP and TCA pathways at the transcriptional level, and alleviated the effects of combined stress on EMP–TCA metabolic processes at the physiological and biochemical levels by increasing PDH, α-KGDH and NAD-MDH in aerial part by 27.22%, 18.85% and 140.37%, HK, PK and PEPC in underground part by 93.97%, 25.81% and 31.19%, initiated the replenishment mechanism and inhibited GABA shunt in underground part of *G. uralensis* to provide energy for vital activities. In conclusion, Si can effectively regulate respiration metabolism process to provide more substrates for subsequent physiological processes, thus improving tolerance to salt and drought stress, and thereby promote the growth of *G. uralensis* seedlings under stress conditions.

Keywords *G. uralensis* seedlings · Respiration · Silicon · Salt or/and drought stress · Transcriptome analysis

Communicated by Mohsin Tanveer.

✉ Enhe Zhang
416483736@qq.com

✉ Xinhui Zhang
zhang2013512@163.com

[1] College of Agronomy, Gansu Agricultural University, Lanzhou 730070, China

[2] College of Pharmacy, Ningxia Medical University, Yinchuan 750004, China

[3] Ningxia Engineering and Technology Research Center of Regional Characterizistic Traditional Chinese Medicine, Ningxia Collaborative Innovation Center of Regional Characterizistic Traditional Chinese Medicine, Key Laboratory of Ningxia Minority Medicine Modernization, Ministry of Education, Yinchuan 750004, China

[4] State Key Laboratory of Aridland Crop Science, Lanzhou 730070, China

Introduction

In the process of natural growth and development, plants inevitably encounter various adverse environmental conditions due to immobility (Liu et al. 2021). Thereinto, drought and salinity, two of the most widespread abiotic stress factors globally, adversely affect the establishment, growth, and development of plants, ultimately leading to reduced crop yield (Du et al. 2020; Zhuang et al. 2021). Moreover, these two abiotic stresses usually occur simultaneously in natural and agricultural ecosystems as the drought may lead to high soil salinity in the soil (Ma et al. 2020). Therefore, for the future development of saline cultivation in arid and semi-arid regions, it is necessary to understand plant stress responses and its response mechanisms under combined stresses, rather than considering only individual stress.

Plants undergo various changes in morphological, physiological, and biological processes to thrive in the harsh stress conditions. For instance, drought usually results in etiolation, atrophy, curling, senescence, and reduced size of leaves, slim and elongation of stem, and deep expansion of root system (Wu et al. 2022), and salinity causes dwarfism, reduced leaf area, and increased root/shoot ratio (R/T) (Ahanger et al. 2020; Shen et al. 2022). Recent studies have found that plants undergo a series of physiological, biochemical, and molecular changes, which ultimately disorder metabolic processes such as respiration in plants under stress conditions (Liu et al. 2020a). Stress-induced oxidative stress can result in the redistribution of glycolytic carbon flux into the PPP (Xu et al. 2022) and perturbation of the EMP pathway-TCA cycle by inhibiting related enzyme activities in the TCA cycle (Li et al. 2020). It is also reported that stress condition can shift TCA cycle to the GABA shunt (Che-Othman et al. 2020). However, maintaining respiration metabolism may play a vital role in plant adaptation to adverse environmental stress conditions (Liu et al. 2020a, b). One ideal solution would be to enhance plant stress tolerance by adding harmless exogenous substances to maintain normal life processes. In recent years, silicon (Si), an environment-friendly element beneficial to plants, has been effectively applied in the field of adversity stress to mitigate the inhibition of stress on plants (Jan et al. 2018).

Silicon plays a crucial role in sustainable agricultural development (Verma et al. 2020). Previous studies revealed that Si application could increase drought and salt tolerance of plants through either a direct or indirect mechanism (Wang et al. 2021; Dhiman et al. 2021). Specifically, Si alleviated the inhibitory effect of drought and salt stress on plant growth in various ways, such as by increasing leaf area and plant height (Shen et al. 2022), enhancing growth of roots (Ahire et al. 2021), and increasing biomass accumulation (Verma et al. 2020). In addition, Si could change the respiration and metabolism pathway of plants under drought and salt stress, including slowing down the TCA cycle by increasing the diversion of acetyl-CoA to lipid biosynthesis (Mundada et al. 2021) and inducing GABA shunt (Das et al. 2021), thus improving tolerance. Therefore, the regulation of respiratory metabolism in plants is one of the important mechanisms by which Si can improve plant tolerance.

As one of the main vegetation resources in arid and semiarid areas worldwide, *Glycyrrhiza Uralensis* Fisch. (*G. uralensis*) has strong drought and salt tolerance, and it plays not only an essential ecological role in soil and water conservation, wind prevention, and sand fixation but also is a traditional medicinal herb in Europe and Asia with great therapeutic value and potential for development (Zhong et al. 2022). Previous studies have shown that stress can increase the content of active ingredients in *G. uralensis* (Yao et al. 2022; Han et al. 2022). However, the seedling stage is extremely sensitive to stress tolerance (Zhang et al. 2022). Thus, it is of great scientific significance to explore the physiological stress process and response mechanism of *G. uralensis* seedlings under adverse conditions in alleviating stress. Previous studies have proved that Si can improve the stress tolerance of *G. uralensis* seedlings by regulating carbon and nitrogen metabolism (Cui et al. 2021). However, the comprehensive regulation mechanisms of Si on respiratory metabolism of *G. uralensis* seedlings under drought, salt, and combined stresses are still unclear. In the present study, the growth properties, respiratory metabolic pathways, and gene expression of *G. uralensis* seedlings were analyzed, which could provide a theoretical basis for using Si application in agriculture.

Materials and methods

Plant materials and growth conditions

The pot experiment was conducted in a constant temperature incubator at the Gansu Agricultural University, Lanzhou City, Gansu Province, China. Seeds were collected from wild *G. uralensis* plants in Urad Front Banner, Inner Mongolia, China, in September 2019, which was identified as *G. uralensis*Fisch. by Professor Xinhui Zhang of Ningxia Medical University. Healthy seeds were selected and stored in a kraft paper bag at 4 °C until use. Seeds were soaked in concentrated H_2SO_4 for 40 min to break the thick seed coat, surface-sterilized for 10 min by soaking in 10% H_2O_2, washed several times with distilled water, and then imbibed with distilled water for 7 h at 4 °C. Using the sand culture method, 60 seeds were sown in plastic pots (with a 9.5 cm

base diameter, 11 cm height, and 13 cm diameter), which were filled with 1000 g of sterilized sand, and then covered with 200 g of sterilized sand. The sand in the pots was kept humid at 70 ± 5% of the field water-holding capacity until the second true leaf was fully developed (approximately 25 days later).

Treatments and experimental design

The experiments had a completely random design, and eight replications were conducted. The *G. uralensis* seedlings were subjected to the following eight treatments: soil relative water content of 70 ± 5% (control, CK); soil relative water content of 40 ± 5% (drought (D) stress); 75 mM NaCl (salt (S) stress); 75 mM NaCl + soil relative water content of 40 ± 5% (salt and drought (S+D) stress); soil relative water content of 70 ± 5% + 2 mM potassium silicate (K_2SiO_3) (CK+Si); soil relative water content of 40 ± 5%+ 2 mM K_2SiO_3 (D+Si); 75 mM NaCl + 2 mM K_2SiO_3 (S+Si); 75 mM NaCl + soil relative water content of 40 ± 5% + 2 mM K_2SiO_3 (S+D+Si). Soil moisture was controlled by weighing, and it was irrigated every two days. All pots were randomly arranged and periodically rotated to minimize the effects of environmental heterogeneity.

After 20 days of stress and Si treatment, plants were collected for subsequent experiments. Generally, eight pots were selected for each treatment. First, three pots were randomly selected for each treatment; all plants in the pots were removed from the soil, and aboveground growth indices were recorded. Next, the root samples were scanned using a scanner (Epson Perfection 4990 Photo type) with a resolution of 300 dpi, and the scanned images were analyzed using Win RHIZO root analysis software to measure characteristic parameters such as root length, surface area, and volume. The samples were then oven-dried at 60 °C for 48 h and weighed. The seedlings from the remaining five pots of each treatment were removed from the soil between 9 and 11 a.m., washed immediately with distilled water, and then a few leaves were randomly collected and mixed to determine chlorophyll (Chl) content, while the rest of the samples were immediately stored at − 80 °C for subsequent determination of enzyme activities.

Determination of key enzyme activities of respiratory metabolism

For the determination of various physiological indicators-associated respiratory metabolism, we used reagent kits (Sino Best Biological Technology Co., Ltd.), which included key enzymes in the EMP : hexokinase (HK), phosphofructokinase (PFK), and pyruvate kinase (PK); key enzymes in the TCA cycle: pyruvate dehydrogenase (PDH), α-ketoglutarate dehydrogenase (α-KGDH), mitochondrial isocitrate dehydrogenase (ICDHm), succinate dehydrogenase (SDH), and malate dehydrogenase (MDH) enzyme activities, as well as acetyl coenzyme A (acetyl-CoA) content; key enzymes in the PPP: glucose-6-phosphate dehydrogenase (G6PDH) and 6-phosphogluconic dehydrogenase (6-PGDH).

The HK activity was determined using glucose as the substrate to record the increase in absorbance at 340 nm cause by the production of NADPH. PFK was determined using fructose-6-phosphate as the substrate to record the decrease in absorbance at 340 nm cause by the enzymatic oxidation of NADH. PK was determined using phosphoenolpyruvate (PEP) as the substrate to record the decrease in absorbance at 340 nm caused by the enzymatic oxidation of NADH. The PDH activity was determined using pyruvate and 2,6-dichlorophenol indophenol (2,6-DCPIP) as the substrate to record the decrease in absorbance at 605 nm. The content of acetyl-CoA was determined by recording the increase in absorbance at 340 nm cause by the production of NADPH using the coupling reaction of malate dehydrogenase and citrate synthase. The α-KGDH activity was determined using α-ketoglutarate as the substrate to record the increase in absorbance at 340 nm cause by the enzymatic reduction of NAD^+, and ICDHm was determined by recording the increase in absorbance at 340 nm. SDH was determined using succinic acid as the substrate to record the reduction rate of 2,6-DCPIP at 600 nm. NAD-MDH was determined using oxaloacetate (OAA) as the substrate to record the decrease in absorbance at 340 nm. The G6PDH and 6-PGDH activity was determined by recording the increase in absorbance at 340 nm caused by the enzymatic reduction of $NADP^+$.

RNA-Seq analysis

The work was conducted by Beijing Baimeike Company (Beijing, China) on an Illumina HiSeq 500 platform. Total RNA from the aerial tissue and underground tissue of *G. uralensis* seedlings collected from eight treatments (CK, CK+Si, S, S+Si, D, D+Si, S+D and S+D+Si) was used for cDNA library construction, with three replicates in each treatment. RNA concentration and purity was measured using NanoDrop 2000 (Thermo Fisher Scientific, Wilmington, DE). RNA integrity was assessed using the RNA Nano 6000 Assay Kit of the Agilent Bioanalyzer 2100 system (Agilent Technologies, CA, USA). Sequencing libraries were constructed using NEBNext UltraTM RNA Library Prep Kit for Illumina (NEB, USA) and sequenced on Illumina platform. HISAT2 was used to map clean reads to reference genome. The read numbers were transformed into the fragments per kilobase of transcript sequence per million base pairs sequenced (FPKM) value for gene expression quantification (Florea et al. 2013). Differentially expressed

genes (DEGs) were identified using DESeq2 package. Gene expression fold change ≥ 1.5 and false discovery rate (FDR) < 0.05 were set as the threshold values for subsequent analysis. GSEA was performed using BMKCloud (www.biocloud.net), pvalue < 0.05 and FDR < 0.25 were set as the threshold values.

Statistical analyses

Statistical analysis was performed using SPSS Statistics 20.0. Differences between means were tested by one-way analysis of variance (ANOVA) using Duncan's multiple range tests, and $p < 0.05$ was considered statistically significant. All treatments have three replication operations presented as the mean ± SD of each experiment. Principal component analysis (PCA) was performed with Canoco 5.0.

Results

Plant growth parameters and root morphological traits

The change in the morphological traits of stressed plant is the most intuitive representation of stresses threatening plant growth. Relative to the CK, salt stress inhibited the growth of *G. uralensis* seedlings by decreasing plant height, leaf number, leaf area, and aboveground biomass by 17.41%, 15.13%, 25.73% and 8.68%, respectively, but increased the main root diameter, underground biomass and R/T significantly by 21.10%, 15.05% and 25.87, respectively (Fig. 1,Table 1); drought stress remarkably declined the stem diameter by 7.36% but increased the lateral root number by 9.24%; combined stress significantly decreased plant height, stem diameter, leaf number, leaf area, total root volume, aboveground biomass, and total biomass by 21.03%, 9.81%, 23.45%, 33.81%, 16.37%, 30.13% and 19.99%, while increased R/T by 34.08%. The S+Si treatment increased leaf number by 15.13%, but decreased the total root length and lateral root number by 11.13% and 17.30%, relative to S alone. The D+Si treatment significantly increased underground biomass by 11.40% but decreased the leaf area and total root volume by 13.39% and 6.92% of D stressed-plants. Additionally, Si increased leaf number and aboveground biomass by 11.96% and 23.88%, but decreased R/T by 11.87% of *G. uralensis* subjected to S+D stress (Fig. 1, Table 1).

EMP metabolism process

Both stress and Si had different effects on aerobic and anaerobic respiration in the EMP pathway. In the aerobic respiration phase, the S, D and S+D treatments significantly increased HK activity by 56.04%, 163.86% and 268.99% in the aerial part of *G. uralensis* seedlings, respectively, relative to CK alone (Figs. 2, 3). In addition, the PFK activity remarkably increased by 73.82% and 34.95% in the aerial part of D and S+D-treated plants (Figs. 2, 3). However, the transcriptional analysis showed no differences in the expression of genes encoding HK in their aerial parts between stress-treated plants and the CK (Fig. 5; Table 2). In addition, salt stress upregulated one gene encoding PFK and downregulated three genes encoding PFK, PK, and GAPDH, respectively. Drought stress upregulated three genes encoding PFK, 2,3-bisphosphoglycerate-dependent phosphoglycerate mutase (PGAM), and PK, respectively. Combined stress upregulated six genes encoding diphosphate-dependent phosphofructokinase (PPi-PFK), GAPDH ($NADP^+$), PGAM, PFK, and PK and downregulated twelve genes encoding PFK, PPi-PFK, GAPDH, PGAM, 2,3-bisphosphoglycerate 3-phosphatase (2,3-BPG 3-phosphatase), enolase, and PK. Silicon addition significantly increased the activity levels of PFK and PK by 18.14% and 44.70% in the aerial part of the seedlings exposed to S. However, the transcriptional analysis showed no differences in the expression of genes in the EMP pathway in the aerial part of *G. uralensis* seedlings between S and S+Si treatments. Compared with D treatment, Si application significantly increased the HK and PK by 84.57% and 27.32% but decreased PFK by 21.76% in their aerial parts. However, the addition of Si downregulated three genes encoding PFK, PGAM, and PK, respectively, in D-treated plants. In S+D+Si-treated seedlings, HK and PFK declined by 74.86% and 57.53%, respectively, relative to S+D-stressed seedlings. However, S+D+Si stress upregulated seven genes encoding HK, PPi-PFK, 2,3-BPG 3-phosphatase, enolase, and PK, and downregulated four genes encoding PFK, PPi-PFK, GAPDH (NADP+), and PK, respectively.

In addition to the genes mentioned above, in the anaerobic respiration phase, the genes encoding pyruvate decarboxylase (PDC), lactate dehydrogenase (LDH), aldehyde dehydrogenase (ALDH), and alcohol dehydrogenase (ADH) in the aerial part of *G. uralensis* were affected by stress or Si (Fig. 5; Table 2). Specifically, two genes encoding ADH upregulated in S_vs_CK comparison, four genes encoding PDC, ALDH, and ADH upregulated and one gene encoding ALDH down-regulated in D_vs_CK comparison, as well as three genes encoding ALDH and ADH downregulated and the other three genes encoding ALDH and ADH upregulated in S+D_vs_CK comparison. However, Si addition had no effect on the genes related to the EMP pathway in the aerial part of *G. uralensis* seedlings under S stress. One gene encoding ALDH downregulated and two genes encoding ALDH and ADH, respectively, upregulated in D+Si_vs_D comparison, as well as five genes encoding PDC, ALDH, and ADH, upregulated and one gene encoding LDH downregulated in S+D+Si_vs_S+D comparison.

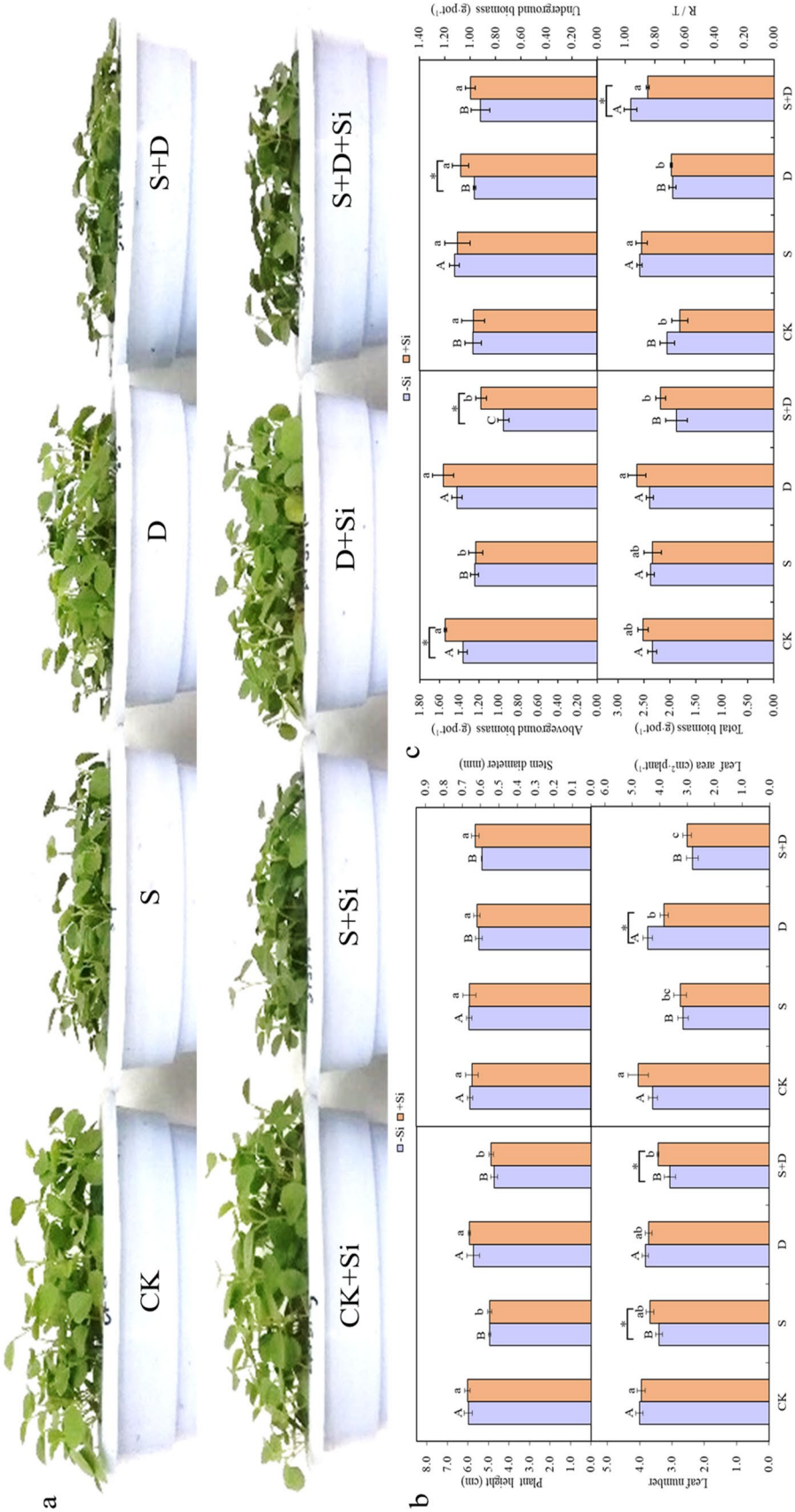


Fig. 1 **a** A part of the experiment layout of *G. uralensis* seedlings grown under different stress without or with Si. Effect of exogenous Si on the growth parameters in aerial part (**b**) and biomass (**c**) of *G. uralensis* seedlings grown under different stress. The different capital letters indicate the significant difference at $p < 0.05$ within the different treatments without Si, the different lowercase letters indicate the significant difference at $p < 0.05$ within the different treatments with Si addition. The " * " stands for the significant difference at $p < 0.05$ between two treatments under absence of Si and application of Si. Error bars represent the standard error

Table 1 Effect of Si on the root morphological trait of *G. uralensis* seedlings under different stress

Treatment	Total root length (cm)		Total surface aera (cm^2)		Total root volume (cm^3)		Main root diameter (mm)		Average root diameter (mm)		Lateral root number	
CK	54.14 ± 2.16 AB	*	7.52 ± 0.34 AB	ns	0.0831 ± 0.0039 A	ns	1.35 ± 0.05 B	ns	0.0874 ± 0.0021 A	*	13.36 ± 0.80 B	*
CK+Si	45.33 ± 2.60 b		6.72 ± 0.38 a		0.0795 ± 0.0056 a		1.26 ± 0.04 bc		0.0945 ± 0.0030 a		11.17 ± 0.95 b	
S	55.31 ± 2.48 AB	*	7.75 ± 0.63 A	ns	0.0856 ± 0.0055 A	ns	1.64 ± 0.06 A	ns	0.0887 ± 0.0017 A	ns	16.41 ± 1.26 AB	*
S+Si	49.15 ± 2.72 ab		6.8 ± 0.40 a		0.0751 ± 0.0026 a		1.57 ± 0.03 a		0.0900 ± 0.0031 ab		13.57 ± 0.80 ab	
D	59.15 ± 2.54 A	ns	7.71 ± 0.41 A	ns	0.0809 ± 0.0049 AB	*	1.29 ± 0.01 B	ns	0.0834 ± 0.0012 A	ns	17.29 ± 0.98 A	ns
D+Si	54.94 ± 2.16 a		7.21 ± 0.36 a		0.0753 ± 0.0049 a		1.22 ± 0.08 c		0.0835 ± 0.0018 b		15.96 ± 1.18 a	
S+D	48.88 ± 2.65 B	ns	6.53 ± 0.51 B	ns	0.0695 ± 0.0042 B	ns	1.37 ± 0.02 B	ns	0.0848 ± 0.0021 A	ns	14.65 ± 0.65 AB	ns
S+D+Si	52.1 ± 1.32 ab		6.72 ± 0.24 a		0.0691 ± 0.0032 a		1.42 ± 0.05 ab		0.0821 ± 0.0010 b		16.41 ± 1.08 a	

Data are shown as mean ± SE. In the same column with different capital letters indicate the significant difference at 0.05 level within different treatments without Si. And in the same column with different lowercase letters indicate the significant difference at 0.05 level within the different treatments with Si. The "*" stands for the significant difference at 0.05 level and ns for not significant difference between two treatments with or without 0.2 mM K_2SiO_3

In the underground part of *G. uralensis* seedlings, salinity significantly increased the HK by 287.92% and decreased PK and PFK by 15.97% and 21.54% over the control (Figs. 2, 3). However, transcriptional analysis showed that S stress downregulated five genes encoding HK, PFK, and PK but upregulated one gene encoding GAPDH ($NADP^+$) (Fig. 5; Table 3). Drought stress greatly increased HK and PK by 234.41% and 76.02%, respectively, but had no effect on genes encoding HK and PK. Besides, one gene encoding GAPDH was downregulated in the underground part of D-treated plants. Combined stress increased the PK by 17.12% and decreased the PFK by 34.75%, and downregulated four genes encoding HK, triosephosphate isomerase (TIM), PFK, and PK, respectively, and upregulated two genes encoding PFK and GAPDH ($NADP^+$), respectively. With the Si addition, the variation trends of HK, PFK, and PK in the underground part were similar to those in the aerial part under S stress conditions, but the values of HK and PK were higher, while that of PFK was lower. Relative to drought-stressed plants, Si addition greatly increased the HK by 53.73% and decreased the activity levels of PK and PFK by 38.11% and 41.58% in the underground part. However, no related genes were differentially expressed in S+Si _vs_S and D+Si_vs_D comparison. The addition of Si increased HK and PK by 93.97% and 25.81% in the underground part of plants subjected to S+D stress and upregulated three genes encoding HK and PGAM.

In the anaerobic respiration phase, S stress upregulated two genes encoding ALDH and ADH, respectively, D stress downregulated one gene encoding PDC, and S+D stress downregulated three genes encoding PDC and ALDH and upregulated eight genes encoding PDC, ADH, and ALDH in the underground part (Fig. 5; Table 3). With the Si addition, one gene encoding PDC upregulated and one gene encoding ADH downregulated in S-treated plants. Si addition had no effect on the related genes in the underground part of *G. uralensis* seedlings under D and S+D stress conditions.

TCA cycle

Relative to control, ICDHm, SDH, and NAD-MDH and the content of acetyl-CoA in the aerial part decreased by 35.77%, 20.93%, 50.13% and 32.75% due to salt stress (Figs. 3, 4). Our transcriptome analysis results showed two genes encoding α-KGDH and SDH downregulated and one gene encoding MDH upregulated in S _vs_ CK comparison (Fig. 5, Table 2). D stress significantly decreased PDH, SDH, and NAD-MDH and the content of acetyl-CoA by 21.53%, 14.31%, 47.83% and 60.65%, respectively, but increased α-KGDH by 58.04% in the aerial part over the control. However, the transcriptional analysis showed that only one gene encoding ICDHm upregulated in D_vs_CK comparison. Under S+D stress, the patterns of variation

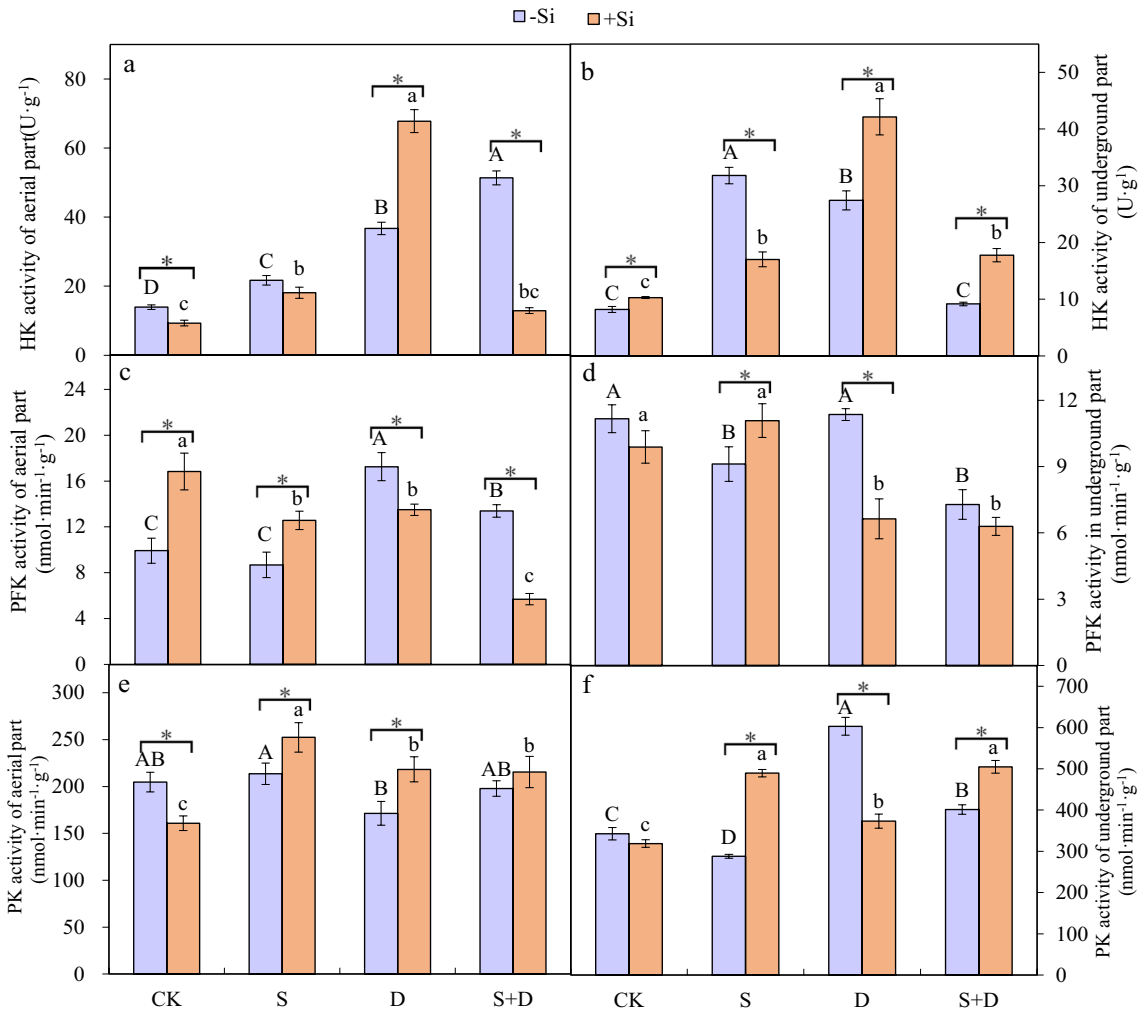


Fig. 2 Effect of exogenous Si on key enzyme activities in EMP pathway in aerial and underground part of *G. uralensis* seedlings grown under different stress. *HK* hexokinase, *PFK* phosphofructokinase, *PK* pyruvate kinase. The different capital letters indicate the significant difference at $p < 0.05$ within the different treatments without Si, the different lowercase letters indicate the significant difference at $p < 0.05$ within the different treatments with Si addition. The " * " stands for the significant difference at $p < 0.05$ between two treatments under absence of Si and application of Si. Error bars represent the standard error

for key enzymes in the TCA cycle in the aerial part were similar to those under D stress. However, the transcriptome results differed, with S+D stress downregulating eight genes encoding PDH, citrate synthase (CS), ICDHm, α-KGDH, SDH, aconitate hydratase, and upregulating one gene encoding MDH. Relative to salt stressed plants, Si addition decreased PDH and NAD-MDH by 27.50% and 67.64% but increased ICDHm, α-KGDH, and the content of acetyl-CoA by 108.71%, 19.71% and 39.97%. Relative to drought stressed plants, Si decreased SDH by 36.3% and increased NAD-MDH and the content of acetyl-CoA by 32.72% and 62.31%. However, transcriptome results showed no differences in S+ Si_vs_S and D+Si_vs_D comparison. Application of Si decreased SDH by 34.56% and increased PDH, α-KGDH, and NAD-MDH by 27.22%, 18.88% and 140.37%, respectively, and upregulated three genes encoding CS and α-KGDH in the aerial part of S+D-treated plants.

Relative to control, ICDHm decreased by 67.04% and PDH, α-KGDH, SDH, and NAD-MDH increased by 166.22%, 46.88%, 61.65% and 71.28%, respectively, in the underground part of salt stressed seedlings (Figs. 3, 4); drought stress decreased ICDHm by 78.73%, but increased PDH, SDH, and NAD-MDH by 50.02%, 116.94% and 44.87%, respectively; combined stress increased PDH, SDH, and NAD-MDH and the acetyl-CoA content 170.87%, 79.45%, 101.14% and 22.11%, while decreased ICDHm and α-KGDH by 70.39% and 38.26%, respectively. However, transcriptome results showed that salt stress downregulated one gene encoding CS and upregulated one gene encoding NAD-MDH; drought stress downregulated two genes

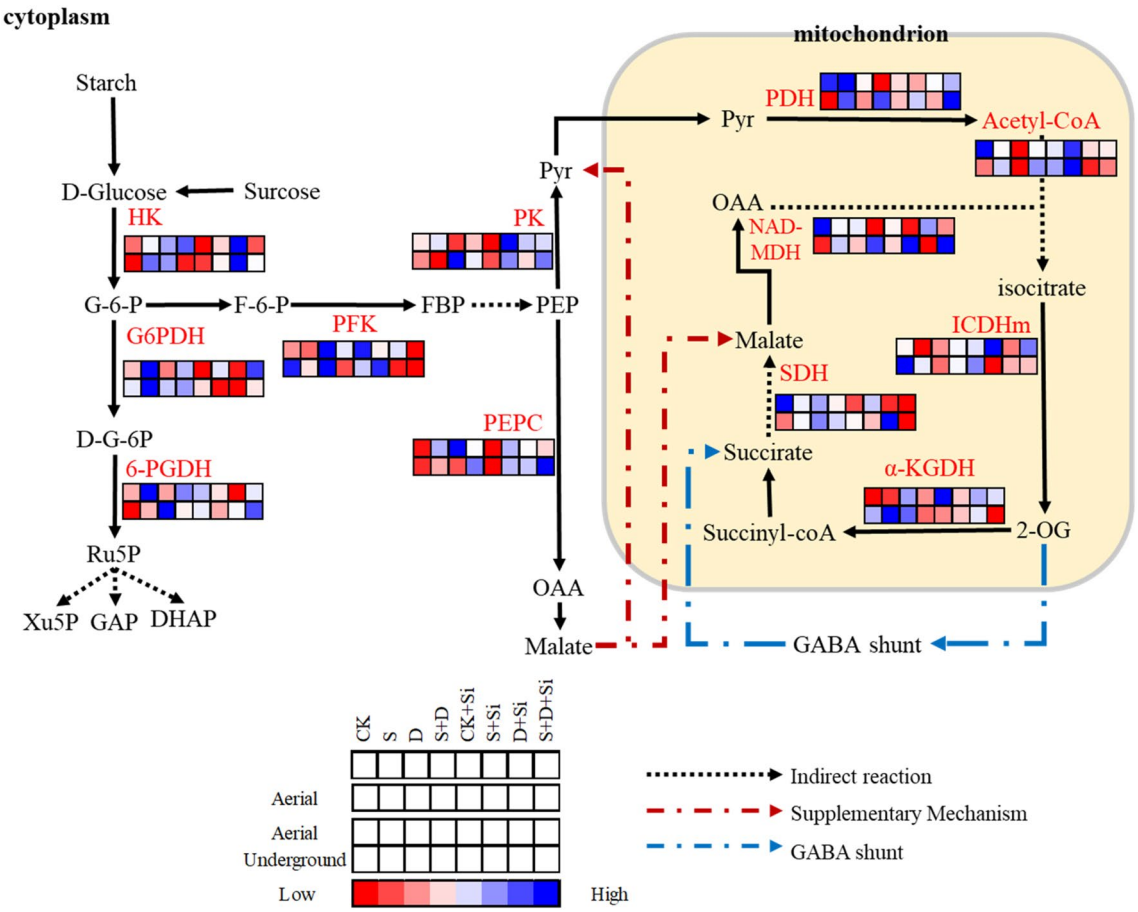


Fig. 3 Effect of exogenous Si on the enzyme activities in respiration metabolism of *G. uralensis* seedlings grown under different stress.*HK* hexokinase, *G-6-P* glucose-6-phosphate, *F-6-P* fructose-6-phosphate, *PFK* phosphofructokinase, *FBP* fructose-1,6-bisphosphate, *PEP* Phosphoenolpyruvate, *PK* pyruvate kinase, *Pyr* pyruvate, *PDH* pyruvate dehydrogenase, *OAA* oxaloacetic acid, *ICDHm* isocitrate dehydrogenase, *2-OG* 2-oxoglutarate, *α-KGDH* 2-oxoglutarate dehydrogenase, *SDH* succinate dehydrogenase, *NAD-MDH* malate dehydrogenase, *G6PDH* glucose-6-phosphate dehydrogenase, *D-G-6P* D-glucose-6-phosphate, *6-PGDH* 6-phosphogluconic dehydrogenase, *Ru5P* ribulose-5-phosphate, *GAP* Glyceraldehyde-3-phosphate, *DHAP* dihydroxyacetone-3-phosphate, *Xu5P* xylulose-5-phosphate

encoding CS and α-KGDH, respectively; combined stress downregulated two genes encoding PDH and CS, respectively, and upregulated one gene encoding NAD-MDH (Fig. 5; Table 3). Relative to salt stressed plants, Si addition decreased PDH, ICDHm, and α-KGDH in the underground part by 20.41%, 49.25% and 50.71%, but increased NAD-MDH and the content of acetyl-CoA in the underground part by 24.16% and 24.86%, respectively. Relative to drought stressed plants, αD-stressed plants, adding Si decreased α-KGDH, SDH, and the acetyl-CoA content in the underground part by 19.89%, 73.54% and 17.93%, respectively. However, Si addition had no effect on genes related to the TCA cycle in their underground part under any stress.

Some intermediates of the TCA cycle are the synthetic precursors for many important organic compounds. The proper functioning of the TCA cycle can be compromised when its intermediates products are consumed in large quantities to synthesize organic compounds. The PEPC enzyme catalyzing PEP to replenish OAA is one of the important complementary mechanisms of the TCA cycle. Under stress conditions, the PEPC in the aerial part increased with S (2.78-fold), D (3.94-fold) and S+D (2.30-fold), respectively, relative to CK. (Fig. 6). However, the transcriptome results were different, with S and S + D stresses downregulating one gene encoding PEPC and D stress having no effect (Fig. 5; Table 2). Si addition greatly decreased PEPC by 42.37% in the aerial part of D-treated plants but had no effect on it of plants under S and S+D stresses. Transcriptome results showed that Si addition had no effect on the genes encoding PEPC in the aerial part of plants under any of the three stresses. As in the aerial part, PEPC in the underground part also increased under stress conditions to varying degrees (Fig. 6). Moreover, Si addition further increased the PEPC in the underground part by 69.07 with S+Si, 145.48% with D+Si and 31.19% with S+D+Si. However, either the stress nor Si addition

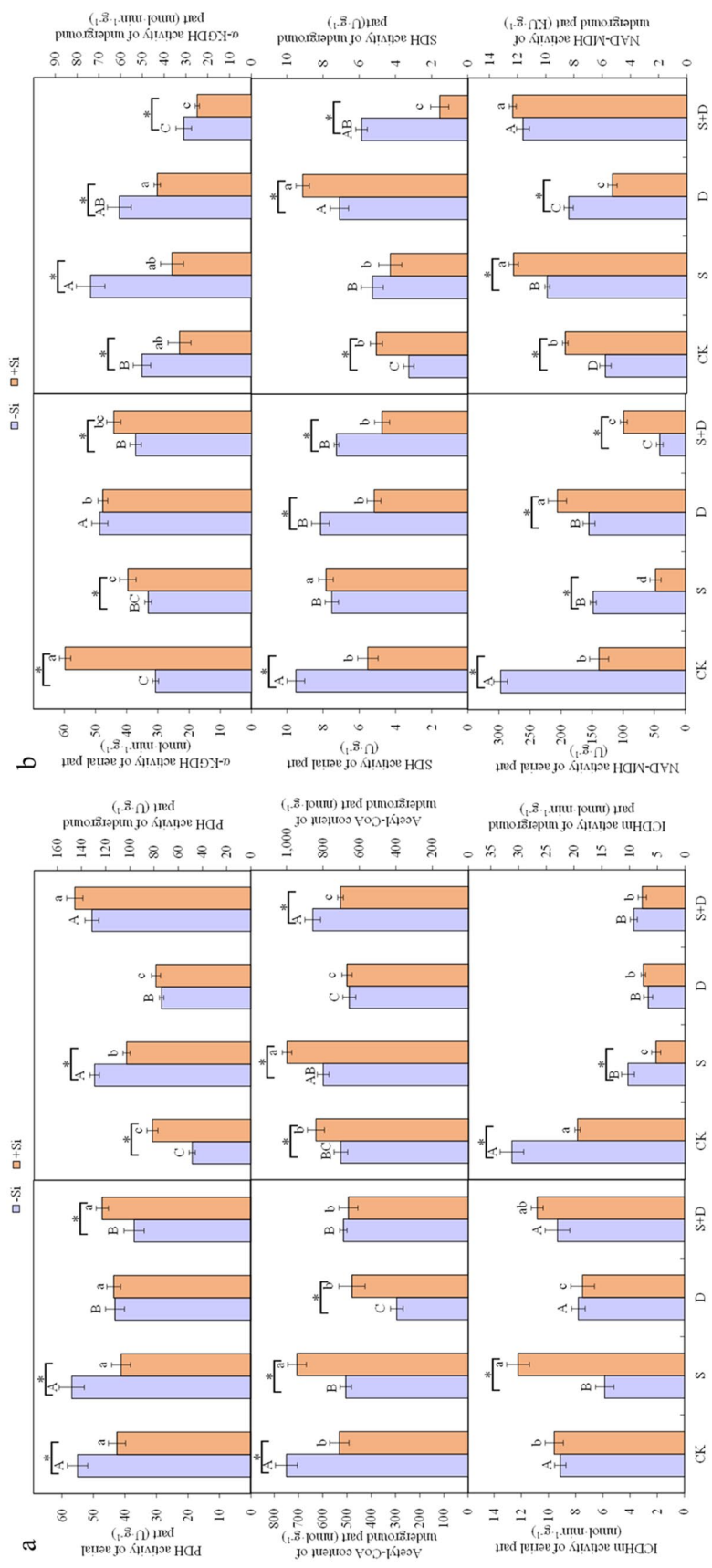
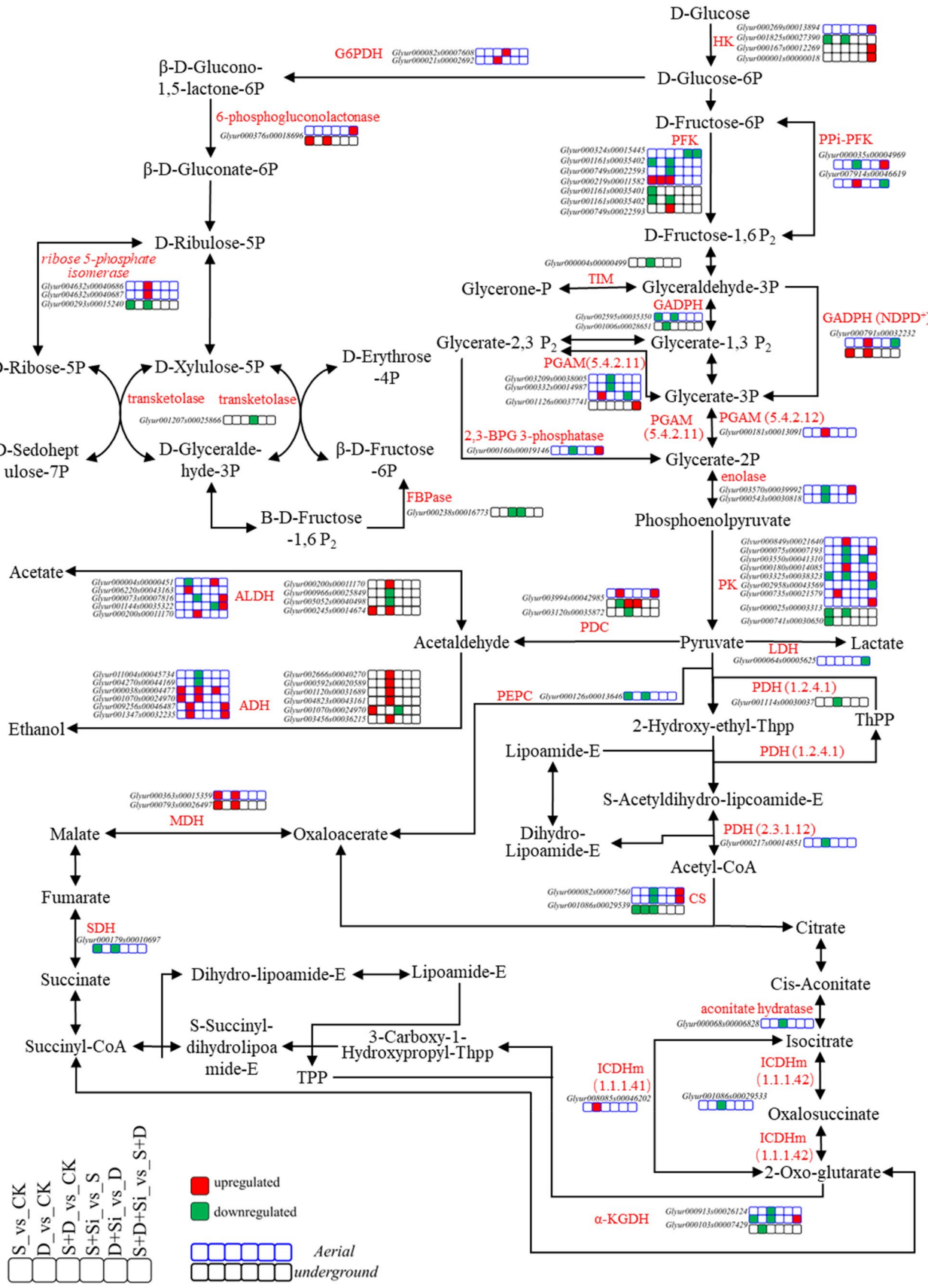


Fig. 4 Effect of exogenous Si on key enzyme activities in TCA cycle in aerial and underground part of *G. uralensis* seedlings grown under different stress. PDH, pyruvate dehydrogenase; ICDHm: isocitrate dehydrogenase; α-KGDH, 2-oxoglutarate dehydrogenase; SDH, succinate dehydrogenase, NAD-MDH, malate dehydrogenase;The different capital letters indicate the significant difference at $p < 0.05$ within the different treatments without Si, the different lowercase letters indicate the significant difference at $p < 0.05$ within the different treatments with Si addition. The " * " stands for the significant difference at $p < 0.05$ between two treatments under absence of Si and application of Si. Error bars represent the standard error


D-Glucose
HK
D-Glucose-6P
G6PDH
β-D-Glucono-
1,5-lactone-6P
6-phosphogluconolactonase
β-D-Gluconate-6P
D-Fructose-6P
PFK
PPi-PFK
D-Fructose-1,6 P2
D-Ribulose-5P
ribose 5-phosphate
isomerase
TIM
Glycerone-P
Glyceraldehyde-3P
GADPH
GADPH (NDPD+)
D-Ribose-5P
D-Xylulose-5P
D-Erythrose
-4P
Glycerate-2,3 P2
Glycerate-1,3 P2
PGAM(5.4.2.11)
transketolase
transketolase
Glycerate-3P
PGAM
(5.4.2.11)
PGAM (5.4.2.12)
D-Sedohept
ulose-7P
D-Glyceralde-
hyde-3P
β-D-Fructose
-6P
2,3-BPG 3-phosphatase
Glycerate-2P
enolase
FBPase
B-D-Fructose
-1,6 P2
Phosphoenolpyruvate
Acetate
ALDH
PK
PDC
Acetaldehyde
Pyruvate
LDH
Lactate
PEPC
PDH (1.2.4.1)
ADH
Ethanol
2-Hydroxy-ethyl-Thpp
ThPP
Lipoamide-E
PDH (1.2.4.1)
S-Acetyldihydro-lipcoamide-E
MDH
Malate
Oxaloacerate
Dihydro-
Lipoamide-E
PDH (2.3.1.12)
Acetyl-CoA
Fumarate
CS
SDH
Citrate
Succinate
Dihydro-lipoamide-E
Lipoamide-E
Cis-Aconitate
aconitate hydratase
S-Succinyl-
dihydrolipoa
mide-E
3-Carboxy-1-
Hydroxypropyl-Thpp
Succinyl-CoA
Isocitrate
ICDHm
(1.1.1.41)
ICDHm
(1.1.1.42)
TPP
Oxalosuccinate
ICDHm
(1.1.1.42)
2-Oxo-glutarate
α-KGDH
S_vs_CK
D_vs_CK
S+D_vs_CK
S+Si_vs_S
D+Si_vs_D
S+D+Si_vs_S+D
upregulated
downregulated
Aerial
underground

◂**Fig. 5** Effect of exogenous Si on the DEGs in respiration of G. uralensis seedlings grown under different stress. *HK* hexokinase, *PFK* phosphofructokinase, *PK* pyruvate kinase, *TIM* triosephosphate isomerase, *GAPDH* Glyceraldehyde-3-phosphate dehydrogenase, *GAPDH*($NADP^+$) glyceraldehyde-3-phosphate dehydrogenase ($NADP^+$), *PGAM* phosphoglycerate mutase, *2,3-BPG 3-phosphatase* 2,3-bisphosphoglycerate 3-phosphatase, *PDC* pyruvate decarboxylase, *ALDH* aldehyde dehydrogenase, *ADH* alcohol dehydrogenase, *LDH* L-lactate dehydrogenase, *PDH* pyruvate dehydrogenase, *CS* citrate synthetase, *ICDHm* isocitrate dehydrogenase, α-KGDH, 2-oxoglutarate dehydrogenase, *SDH* succinate dehydrogenase, *MDH* malate dehydrogenase, *G6PDH* glucose-6-phosphate dehydrogenase, *FBPase* fructose-1,6-bisphosphatase

affected the genes encoding PEPC in the underground part of *G. uralensis* seedlings (Fig. 5; Table 3).

PPP metabolism process

Relative to control, salt stress greatly increased G6PDH and 6-PGDH in the aerial part by 73.97% and 171.91% (Fig. 7); drought stress had less effect on these; combined stress increased G6PDH and 6-PGDH in the aerial part by 25.56% and 101.12%. Transcriptome results showed that S and D stresses did not affect genes related to the PPP, while S+D stresses upregulated three genes encoding G6PDH and ribose 5-phosphate isomerase (Fig. 5; Table 2). Si addition decreased G6PDH and 6-PGDH in the aerial part by 34.10% and 55.54% with S+Si, 13.22% and 72.93% with D+Si. However, transcriptome results showed that one gene encoding G6PDH was upregulated in S+Si-treated plants, but there was no difference in D+Si_vs_D comparison. Relative to S+D, Si significantly increased G6PDH by 25.77%, decreased 6-PGDH by 28.02%, and upregulated one gene encoding 6-phosphogluconolactonase in the aerial part of *G. uralensis* seedlings.

Relative to control, salt stress increased G6PDH and 6-PGDH in the underground part by 72.88% and 159.47% (Fig. 7). However, the transcriptome results showed that one gene encoding 6-phosphogluconolactonase was upregulated and one gene encoding ribose 5-phosphate isomerase was downregulated in S_vs_CK comparison (Fig. 5; Table 3). Drought stress increased 6-PGDH in the underground part by 845.98% but had no effect on the genes related to the PPP. Combined stress increased G6PDH and 6-PGDH in the underground part by 24.15% and 208.21%. However, two genes encoding FBP and ribose 5-phosphate isomerase, respectively, were downregulated, while one gene encoding 6-phosphogluconolactonase was upregulated in S+D_vs_CK comparison. Si addition significantly decreased G6PDH in the underground part by 83.86% with S+Si, 77.00% with D+i and 30.56% with S+D+Si. Additionally, 6-PGDH in the underground part decreased by 64.71% with D+Si and increased by 144.56% with S+D+Si. However, the transcriptome results showed that two genes encoding FBP and transketolase, respectively, were downregulated in S+Si_vs_S comparison, while there were no significant differences in D+Si_vs_D and S+D+Si_vs_S+D comparison.

Principal component analysis (PCA)

The results of PCA related to plant growth parameters and root morphological traits that we measured revealed a closer association between biological replicates than between stresses or Si treatments (Fig. 8a, b). PC1 explaining 45.97% of total variation uncovered differences between plants of CK and S treatments, CK and S+D treatments, while PC2, accounting for 30.14% of total variation, distinctly separated the plants provided with CK and D treatments, as well as S and S+Si treatments, D and D+Si treatments, and S+D and S+D+Si treatments. PC1 formation covered R/T, leaf area, plant height, leaf number, while PC2 formation covered total root length, lateral root number.

The results of PCA related to EMP pathway, TCA cycle and PPP indexs also revealed a relatively closer association between biological replicates than between stresses or Si treatments (Fig. 8c, d). PC1 explaining 32.49% of total variation revealed differences between plants of CK and S treatments, CK and D treatments, CK and S+D treatments, as well as S and S+Si treatments, and S+D and S+D+Si treatments, while PC2 accounting for 23.45% of total variation distinctly separated the plants provided with D and D+Si treatments. PC1 formation covered PEPC activity in both aerial and underground part, ICDHm activity in underground part, while PC2 formation covers the MDH activity in both aerial and underground part, 6-PGDH activity in aerial part and SDH activity in underground part.

Gene set enrichment analysis (GSEA)

The GSEA of respiration-associated pathways (ko00010: Glycolysis/Gluconeogenesis, ko00020: Citrate cycle, ko00030: Pentose phosphate pathway) were performed to ascertain the function changes in response to stress or Si addition (Fig. 9). In S-U_vs_CK-U comparison (Fig. 9a) and S+D-U_vs_CK-U comparison (Fig. 9b), the TCA cycle (KEGG pathway) were significantly enriched and downregulated. However, in S+Si_vs_S comparison, the TCA cycle were significantly enriched and upregulated in both aerial and underground parts (Fig. 9c, d). Besides, in the S+D+Si_vs_S+D comparison, both EMP and TCA pathways were significantly enriched in the aerial and underground parts, and the overall pathway was upregulated (Fig. 9e–h).

Table 2 Regulation of respiration metabolism-related DEGs in aerial part of *G. uralensis* seedlings by different stress or Si

	Enzyme name	Gene ID	S _vs_ CK	D _vs_ CK	S + D _vs_ CK	S + Si _vs_ S	D + Si _vs_ D	S + D + Si _vs_ S + D	Despection
EMP pathway	*HK*	Glyur000269s00013894	–	–	–	–	–	Up	Hexokinase [EC:2.7.1.1]
	PFK	Glyur000324s00015445	–	–	–	–	Down	Down	6-Phosphofructokinase 1 [EC:2.7.1.11]
	PFK	Glyur001161s00035402	Down	–	Down	--	--	--	6-Phosphofructokinase 1 [EC:2.7.1.11]
	PFK	Glyur000749s00022593	–	–	Down	–	–	–	6-Phosphofructokinase 1 [EC:2.7.1.11]
	PFK	Glyur000219s00011582	Up	Up	Up	–	–	–	6-Phosphofructokinase 1 [EC:2.7.1.11]
	PPi-PFK	Glyur000035s00004969	–	–	Down	–	–	Up	Diphosphate-dependent phosphofructokinase [EC:2.7.1.90]
	PPi-PFK	Glyur007914s00046619	–	–	Up	–	–	Down	Diphosphate-dependent phosphofructokinase [EC:2.7.1.90]
	GADPH (NDPD$^+$)	Glyur000791s00032232	–	–	Up	–	–	Down	Glyceraldehyde-3-phosphate dehydrogenase (NADP+) [EC:1.2.1.9]
	GADPH	Glyur002595s00035350	Down	–	Down	–	–	–	Glyceraldehyde 3-phosphate dehydrogenase [EC:1.2.1.12]
	PGAM	Glyur001126s00037741	–	Up	–	–	Down	–	2,3-Bisphosphoglycerate-dependent phosphoglycerate mutase [EC:5.4.2.11]
	PGAM	Glyur003209s00038005	–	–	Down	–	–	–	2,3-Bisphosphoglycerate-dependent phosphoglycerate mutase [EC:5.4.2.11]
	PGAM	Glyur000332s00014987	–	–	Down	–	–	–	2,3-Bisphosphoglycerate-dependent phosphoglycerate mutase [EC:5.4.2.11]
	PGAM	Glyur000181s00013091	–	–	Up	–	–	–	Phosphoglycerate mutase [EC:5.4.2.12]
	2,3-BPG 3-phosphatase	Glyur000160s00019146	–	–	Down	–	–	Up	2,3-Bisphosphoglycerate 3-phosphatase [EC:3.1.3.80]
	Enolase	Glyur003570s00039992	–	–	Down	–	–	Up	Enolase [EC:4.2.1.11]
	Enolase	Glyur000543s00030818	–	–	Down	–	–	–	Enolase [EC:4.2.1.11]
	PK	Glyur000849s00021640	–	–	Up	–	–	–	Pyruvate kinase [EC:2.7.1.40]
	PK	Glyur000075s00007193	–	–	Down	–	–	Up	Pyruvate kinase [EC:2.7.1.40]
	PK	Glyur003550s00041310	–	–	Down	–	Down	–	Pyruvate kinase [EC:2.7.1.40]
	PK	Glyur000025s00003313	–	–	–	–	–	Up	Pyruvate kinase [EC:2.7.1.40]
	PK	Glyur000180s00014085	–	–	Up	–	–	–	Pyruvate kinase [EC:2.7.1.40]
	PK	Glyur003325s00038323	Down	–	Down	–	–	Up	Pyruvate kinase [EC:2.7.1.40]
	PK	Glyur002958s00043569	–	–	–	–	–	Down	Pyruvate kinase [EC:2.7.1.40]

Table 2 (continued)

	Enzyme name	Gene ID	S _vs_ CK	D _vs_ CK	S + D _vs_ CK	S + Si _vs_ S	D + Si _vs_ D	S + D + Si _vs_ S + D	Despection
	PK	Gly-ur000735s00021579	–	Up	–	–	–	–	Pyruvate kinase [EC:2.7.1.40]
	PDC	Gly-ur003994s00042985	–	Up	–	–	–	Up	Pyruvate decarboxylase [EC:4.1.1.1]
	LDH	Gly-ur000064s00005625	–	–	–	–	–	Down	L-lactate dehydrogenase [EC:1.1.1.27]
	ALDH	Gly-ur000004s00000451	–	Down	–	–	Up	–	Aldehyde dehydrogenase (NAD+) [EC:1.2.1.3]
	ALDH	Gly-ur000200s00011170	–	–	Up	–	–	–	Aldehyde dehydrogenase (NAD+) [EC:1.2.1.3]
	ALDH	Gly-ur006220s00043163	–	Up	–	–	–	–	Aldehyde dehydrogenase (NAD+) [EC:1.2.1.3]
	ALDH	Gly-ur000073s00007816	–	–	Down	–	–	Up	Aldehyde dehydrogenase (NAD+) [EC:1.2.1.3]
	ALDH	Gly-ur001144s00035322	–	–	–	–	Down	Up	Aldehyde dehydrogenase (NAD+) [EC:1.2.1.3]
	ADH	Gly-ur011004s00045734	–	–	Down	–	–	–	Alcohol dehydrogenase [EC:1.1.1.1]
	ADH	Gly-ur004270s00044169	–	–	Down	–	–	–	Alcohol dehydrogenase [EC:1.1.1.1]
	ADH	Gly-ur000038s00004477	Up	–	Up	–	Up	–	Alcohol dehydrogenase [EC:1.1.1.1]
	ADH	Gly-ur001070s00024970	Up	–	Up	–	–	–	Alcohol dehydrogenase class-P [EC:1.1.1.1]
	ADH	Gly-ur009256s00046487	–	Up	–	–	–	Up	Alcohol dehydrogenase class-P [EC:1.1.1.1]
	ADH	Gly-ur001347s00032235	–	Up	–	–	–	Up	Alcohol dehydrogenase class-P [EC:1.1.1.1]
TCA cycle	*PDH*	Gly-ur000217s00014851	–	–	Down	–	–	–	Pyruvate dehydrogenase E2 component (dihydrolipoamide acetyltransferase) [EC:2.3.1.12]
	CS	Gly-ur000082s00007560	–	–	Down	–	–	Up	ATP citrate synthase [EC:2.3.3.8]
	CS	Gly-ur001086s00029539	–	–	Down	–	–	Up	ATP citrate synthase [EC:2.3.3.8]
	ICDHm	Gly-ur001086s00029533	–	–	Down	–	–	–	Isocitrate dehydrogenase [EC:1.1.1.42]
	ICDHm	Gly-ur008085s00046202	–	Up		–	–	–	Isocitrate dehydrogenase (NAD+) [EC:1.1.1.41]
	α-KGDH	Gly-ur000913s00026124	–	–	Down	–	–	–	2-oxoglutarate dehydrogenase E1 component [EC:1.2.4.2]
	α-KGDH	Gly-ur000103s00007429	Down	–	Down	–	–	Up	2-oxoglutarate dehydrogenase E1 component [EC:1.2.4.2]
	SDH	Gly-ur000179s00010697	Down	–	Down	–	–	–	Succinate dehydrogenase (ubiquinone) flavoprotein subunit [EC:1.3.5.1]
	Aconitate hydratase	Gly-ur000068s00006828		–	Down	–	–	–	Aconitate hydratase [EC:4.2.1.3]
	MDH	Gly-ur000363s00015359	Up	–	Up	–	–	–	Malate dehydrogenase [EC:1.1.1.37]
	PEPC	Gly-ur000126s00013646	Down	–	Down	–	–	–	Phosphoenolpyruvate carboxykinase (ATP) [EC:4.1.1.49]

Table 2 (continued)

	Enzyme name	Gene ID	S _vs_ CK	D _vs_ CK	S + D _vs_ CK	S + Si _vs_ S	D + Si _vs_ D	S + D + Si _vs_ S + D	Despection
PPP pathway	*G6PDH*	Glyur000082s00007608	–	–	–	Up	–	–	Glucose-6-phosphate 1-dehydrogenase [EC:1.1.1.49 1.1.1.363]
	G6PDH	Glyur000021s00002692	–	–	Up	–	–	–	Glucose-6-phosphate 1-dehydrogenase [EC:1.1.1.49 1.1.1.363]
	6-Phosphogluconolactonase	Glyur000376s00018696	–	–	–	–	–	Up	6-phosphogluconolactonase [EC:3.1.1.31]
	Ribose 5-phosphate isomerase	Glyur004632s00040686	–	–	Up	–	–	–	Ribose 5-phosphate isomerase A [EC:5.3.1.6]
	ribose 5-phosphate isomerase	Glyur004632s00040687	–	–	Up	–	–	–	Ribose 5-phosphate isomerase A [EC:5.3.1.6

Discussion

Effect of exogenous Si on growth characteristics of *G. uralensis* seedlings grown under different stresses

As the climate continues to deteriorate, the agricultural ecosystems of the contemporary world are under severe stress and challenges. Drought and salt stresses are two major challenges for ecosystems, which hinder plant growth, development, and metabolic processes (Malik et al. 2021). Previous studies have reported that the growth of shoots and roots are significantly inhibited under salt stress (continuous irrigation with 50 mmol NaCl), drought stress (30–35% FWC), and combined stress, thus resulting in less biomass (Egamberdieva et al. 2021; Xie et al. 2019; Zhang et al. 2018). Interestingly, Si addition could ameliorate adverse effects of salt and drought stresses on *G. uralensis* seedlings (Zhang et al.,2020). In this study, salt stress severely inhibited the shoot growth but increased underground biomass (Fig. 1), the change in growth attributes was due to more assimilates allocated to the root system allowing seedlings to survive under S stress condition. The reduction in the stem diameter and increased number of lateral roots of D-stressed *G. uralensis* was observed, which could result in more water uptake and increase in stem hydraulic capacitance to resist stress (El-Katony et al. 2017; Verbeke et al. 2023). Combined stress significantly lowered biomass in both aerial and underground parts but increased R/T ratio due to the superposition effect. Based on the results of PCA, it can be judged that salt stress played a dominant role in combined stress. Si application significantly increased leaf number of S-stress plants, causing larger cover and abundant sunlight for growth, this is consistent with the results of Shen et al. (2022). As for D stress, Si addition decreased leaf area contributing to the reduction in transpiration water loss, which was also observed in soybean by Hussain et al. (2021). As with S stress, Si addition remarkably increased the leaf number of S+D-stress seedlings. In addition, Si addition improved the plant height, stem diameter, and leaf area to varying degrees. Surprisingly, these changes worked in concert to increase the aboveground biomass, thus alleviating the damage on the aerial part of plants under combined stresses.

Effect of exogenous Si on respiration of *G. uralensis* seedlings grown under different stresses

Plants have a variety of respiratory metabolic pathways to adapt to environmental changes, including EMP, TCA, and PPP. The EMP -TCA pathway serves as the primary pathway in the aerobic respiration of plants under normal conditions, providing energy and metabolites needed for plant growth and development (Li et al. 2020). However, the proportion of respiratory pathways in plants under stress conditions may change (Chen et al. 2021).

EMP pathway

HK, PFK, and PK catalyze rate-limiting steps in the EMP pathway, and their decreased activities can inhibit the EMP pathway (Zhong et al. 2016). HK catalyzes the conversion

Table 3 Regulation of respiration metabolism-related DEGs in underground part of *G. uralensis* seedlings by different stress or silicon

	Enzyme name	Gene ID	CK_ vs_S	CK_ vs_D	CK_ vs_S + D	S_ vs_S + Si	D_ vs_D + Si	S + D_ vs_S + D + Si	Despection
EMP pathway	*HK*	Glyur001825s00027390	Down	–	Down	–	–	–	Hexokinase [EC:2.7.1.1]
	HK	Glyur000167s00012269	–	–	–	–	–	Up	Hexokinase [EC:2.7.1.1]
	HK	Glyur000001s00000018	–	–	–	–	–	Up	Hexokinase [EC:2.7.1.1]
	PFK	Glyur001161s00035401	Down	–	–	–	–	–	6-Phosphofructokinase 1 [EC:2.7.1.11]
	PFK	Glyur001161s00035402	Down	–	Down	–	–	–	6-Phosphofructokinase 1 [EC:2.7.1.11]
	PFK	Glyur000749s00022593	–	–	Up	–	–	–	6-Phosphofructokinase 1 [EC:2.7.1.11]
	TIM	Glyur000004s00000499	–	–	Down	–	–	–	Triosephosphate isomerase (TIM) [EC:5.3.1.1]
	GADPH (NDPD+)	Glyur000791s00032232	Up	–	Up	–	–	–	Glyceraldehyde-3-phosphate dehydrogenase (NADP+) [EC:1.2.1.9]
	GADPH	Glyur001006s00028651	–	Down	–	–	–	–	Glyceraldehyde 3-phosphate dehydrogenase [EC:1.2.1.12]
	PGAM	Glyur001126s00037741	–	–	–	–	–	Up	2,3-Bisphosphoglycerate-dependent phosphoglycerate mutase [EC:5.4.2.11]
	PK	Glyur000741s00030650	Down	–	–	–	–	–	Pyruvate kinase [EC:2.7.1.40]
	PK	Glyur000025s00003313	Down	–	Down	–	–	–	Pyruvate kinase [EC:2.7.1.40]
	PDC	Glyur003994s00042985	–	Down	Up	Up	–	–	Pyruvate decarboxylase [EC:4.1.1.1]
	PDC	Glyur003120s00035872	–	–	Down	–	–	–	Pyruvate decarboxylase [EC:4.1.1.1]
	ALDH	Glyur000200s00011170	–	–	Up	–	–	–	Aldehyde dehydrogenase (NAD+) [EC:1.2.1.3]
	ALDH	Glyur000966s00025849	–	–	Down	–	–	–	Aldehyde dehydrogenase (NAD+) [EC:1.2.1.3]
	ALDH	Glyur005052s00040498	–	–	Down	–	–	–	Aldehyde dehydrogenase (NAD+) [EC:1.2.1.3]
	ALDH	Glyur000245s00014674	Up	–	Up	–	–	–	Aldehyde dehydrogenase (NAD+) [EC:1.2.1.3]
	ADH	Glyur002666s00040270	–	–	Up	–	–	–	Alcohol dehydrogenase class-P [EC:1.1.1.1]
	ADH	Glyur000592s00020589	–	–	Up	–	–	–	Alcohol dehydrogenase [EC: 1.1.1.1]
	ADH	Glyur001120s00031689	–	–	Up	–	–	–	Alcohol dehydrogenase [EC: 1.1.1.1]

Table 3 (continued)

	Enzyme name	Gene ID	CK_ vs_S	CK_ vs_D	CK_ vs_S + D	S_ vs_S + Si	D_ vs_D + Si	S + D_ vs_S + D + Si	Despection
	ADH	Gly-ur004823s00043161	–	–	Up	–	–	–	Alcohol dehydrogenase class-P [EC:1.1.1.1]
	ADH	Gly-ur001070s00024970	Up	–	–	Down	–	–	Alcohol dehydrogenase class-P [EC:1.1.1.1]
	ADH	Gly-ur003456s00036215	–	–	Up	–	–	–	Alcohol dehydrogenase class-P [EC:1.1.1.1]
TCA cycle	*PDH*	Gly-ur001114s00030037	–	–	Down	–	–	–	Pyruvate dehydrogenase E1 component beta subunit [EC:1.2.4.1]
	CS	Gly-ur001086s00029539	Down	Down	Down	–	–	–	ATP citrate (pro-S)-lyase [EC:2.3.3.8]
	α-KGDH	Gly-ur000103s00007429	–	Down	–	–	–	–	2-Oxoglutarate dehydrogenase E1 component [EC:1.2.4.2]
	MDH	Gly-ur000793s00026497	Up	–	Up	–	–	–	Malate dehydrogenase [EC:1.1.1.37]
PPP pathway	*FBP*	Gly-ur000238s00016773	–	–	Down	Down	–	–	Fructose-1,6-bisphosphatase I [EC:3.1.3.11]
	6-phosphogluconolactonase	Gly-ur000376s00018696	Up	–	Up	–	–	–	6-Phosphogluconolactonase [EC:3.1.1.31]
	ribose 5-phosphate isomerase	Gly-ur000293s00015240	Down	–	Down	–	–	–	Ribose 5-phosphate isomerase A [EC:5.3.1.6]
	transketolase	Gly-ur001207s00025866	–	–	–	Down	–	–	Transketolase [EC:2.2.1.1]

of glucose into glucose 6-phosphate (G-6-P), which is the intersection of the EMP and PPP (Fig. 3). Li et al. (2020) reported that the HK activity was decreased by salt stress in cucumber; however, Zhong et al. (2016) found the vice versa effect. In this study, S stress significantly increased HK enzyme activity in both aerial and underground parts of *G. uralensis* seedlings to accelerate catabolic metabolism of hexoses, which provided more G-6-P for the EMP pathway and PPP. However, salt stress had no effect on PFK and PK in the aerial part, but decreased them by downregulation of four genes encoding PFK and PK in underground part, to disorder the glycolysis metabolism (Zhong et al. 2016; Li et al. 2020), thereby the elevated G-6-P generated by increased HK might be principally used by the PPP. Drought stress significantly increased HK in both aerial and underground parts of *G. uralensis* seedlings, contributing to high levels of phosphorylation of hexose and the regulation of ROS production (Poór et al. 2019). Besides, drought stress significantly increased PFK and upregulated two genes encoding PFK and PGAM to accelerate the EMP pathway in aerial part, and enhanced PK in the underground part, thus producing more pyruvate for the TCA cycle, thereby improving drought tolerance (Li et al. 2020). Transcriptomic analysis showed 18 DEGs in aerobic respiration phase of the EMP pathway in the aerial part of S+D-treated plants, suggesting that combined stresses evoked a stronger response in the EMP process. Combined stress increased HK and PFK in the aerial part to facilitate the first half of the EMP process, but downregulated nine genes encoding enzymes involved in the reaction from FBP to PEP in the EMP pathway, including GAPDH, phosphoglycerate mutase (PGAM), 2,3-bisphosphoglycerate 3-phosphatase (2,3-BPG 3-phosphatase), and enolase, slowing down the second half of the EMP pathway. Combined stress increase PK in underground part to provide more substrate for the TCA cycle.

In this study, Si addition alleviated the effects of salt stress on HK, which indicated that Si addition diverted hexoses from catabolic reactions to osmotic adjustment, thereby improving the salt tolerance by promoting soluble sugar accumulation (Poór et al. 2011). Besides, Si addition significantly increased PFK and PK in both aerial and underground parts of S-treated seedlings, indicating that Si addition improved the salt tolerance of plants by promoting the EMP process and providing energy and substrate for subsequent life activities of plants (Xiao et al. 2022). However, this also implied that more G-6-P were preserved in the EMP pathway under S stress after Si addition, thus reducing the supply to the PPP. Unlike S stress, Si addition further increased HK in both organs of D-treated seedlings, which was important to ensure a more efficient metabolism of hexoses and that more energy was produced to combat stress. Meanwhile, Si addition significantly decreased PFK activity by downregulation of relative gene in the aerial part, and decreased PFK and PK activities in underground part of D-stressed seedlings to slow-down the EMP process. The results indicated that Si addition alleviated the effects of D stress on EMP process, it was a symbol that Si addition alleviated drought stress. In addition, Si mitigated the effect of S+D stress on the EMP pathway in aerial part by decreasing HK and PFK at physiological and biochemical level and regulating relative genes at the transcriptional level. The decrease in HK could result in soluble sugar accumulation, which was conducive to regulating the cellular osmotic pressure and membrane stabilization (Weiszmann et al. 2018). However, Si addition further increased HK and PK to accelerate the EMP pathway in the underground part of *G. uralensis* seedlings subjected to S+D stress, which is consistent with the GSEA results that the EMP pathway was significantly enriched in both aerial and underground parts, and the overall pathway was upregulated (Fig. 9e, g).

In the absence of oxygen, pyruvate is allocated to anaerobic metabolic pathways for energy production and recycling of NAD^+, thus maintaining the EMP progress with sufficient NAD^+ to provide ATP for plant life (Igamberdiev 2021). Pyruvate is catalyzed to lactate by lactate dehydrogenase (LDH) or acetaldehyde by pyruvate decarboxylase (PDC), both harmful to plants cells. The acetaldehyde is then transformed to acetate by aldehyde dehydrogenase (ALDH) or ethanol by alcohol dehydrogenase (ADH). Ethanol, which is harmless to plants, is easily diffused into the external environment through the lipid bilayer of the cell membrane (Zhou et al. 2017). Our transcriptomic analysis determined that stress and Si addition regulated the genes encoding enzymes related to anaerobic metabolic pathways in both parts of *G. uralensis* seedlings in varying degrees. Specifically, S stress upregulated relative genes encoding ADH or/and ALDH in both aerial and underground part to accelerate the transformation of harmful acetaldehyde to ethanol and acetate. D stress evoked anaerobic respiration to promote NAD^+ regeneration to satisfy the demand for EMP pathway by upregulating relative genes encoding PDC ALDH, and ADH in the aerial parts, but inhibited anaerobic metabolism by downregulating one gene encoding PDC in the underground part. Combined stresses had a greater effect on the anaerobic respiration, wherein six and eleven DEGs were enriched in the anaerobic respiration pathway in the aerial and underground parts, respectively.

Si addition upregulated one gene encoding PDC to promote anaerobic respiration and downregulated one gene encoding ADH to promote more conversion of acetaldehyde to acetate to resist salt stress in the underground part of S-treated seedling (Xiao et al. 2022; Tagnon and Simeon 2017). Si addition further upregulated two genes encoding ALDH and ADH, respectively, to accelerate the transformation of acetaldehyde in the aerial parts of D-treated seedling, thus protecting cells from damage by excessive accumulation of acetaldehyde. In addition, Si addition also promoted anaerobic metabolism by upregulating the genes encoding PDC, ALDH, and ADH in the aerial parts of plants under S+D stresses. Interestingly, Si addition downregulated LDH in the aerial parts of S+D-treated plants, which may prevent cytoplasmic acidification and pH reduction resulting from excessive accumulation of lactate (Zhou et al. 2017) and promote acetate synthesis to withstand stress.

Overall, Si addition alleviated the effects of stress on the EMP of *G. uralensis* seedlings in different ways, with specific mitigation methods varying with stresses. Generally, under salt stress conditions, Si addition diverted hexoses from catabolic reactions to osmotic adaptation, thereby decreased HK activities, and accelerated EMP pathway due to increased PFK and PK activities and upregulation of EMP in transcriptional level. Under drought stress conditions, Si addition further increased HK activity, enhanced hexose catabolism to provide energy and inhibited ROS production. Si alleviated the elevated energy requirements of plants from exposure to drought, thereby decreased PFK and PK activities to slow-down EMP pathway. Also, Si accelerated acetaldehyde conversion by regulating related genes in aerial part to avoid its excessive accumulation induced by D stress. In addition, Si mitigated the effect of S+D stress on the EMP pathway at the transcriptional level by regulating genes and at the physiological and biochemical level by regulating HK and PK activities.

TCA cycle

Pyruvate enters the mitochondria under aerobic conditions and is catalyzed by PDH to generate acetyl-CoA, which links EMP and TCA. In this study, S stress decreased

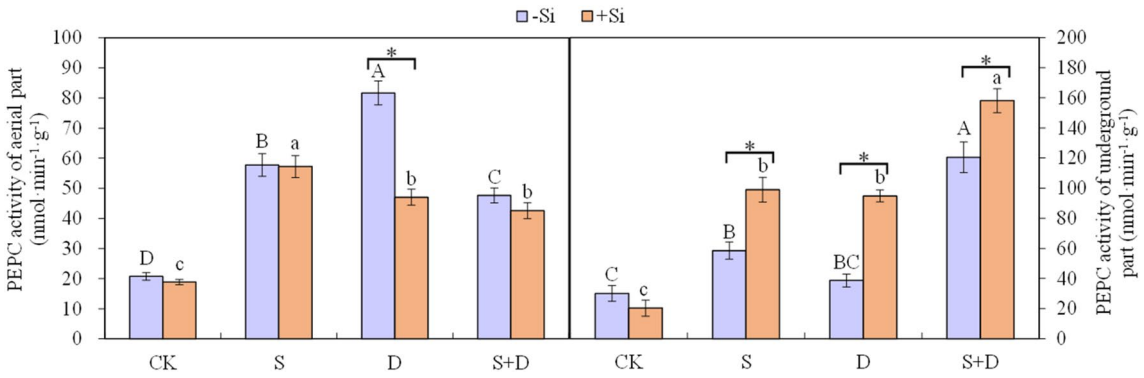


Fig. 6 Effect of exogenous Si on the PEPC activity in aerial and underground part of *G. uralensis* seedlings grown under different stress. The different capital letters indicate the significant difference at $p < 0.05$ within the different treatments without Si, the different lowercase letters indicate the significant difference at $p < 0.05$ within the different treatments with Si addition. The " * " stands for the significant difference at $p < 0.05$ between two treatments under absence of Si and application of Si. Error bars represent the standard error

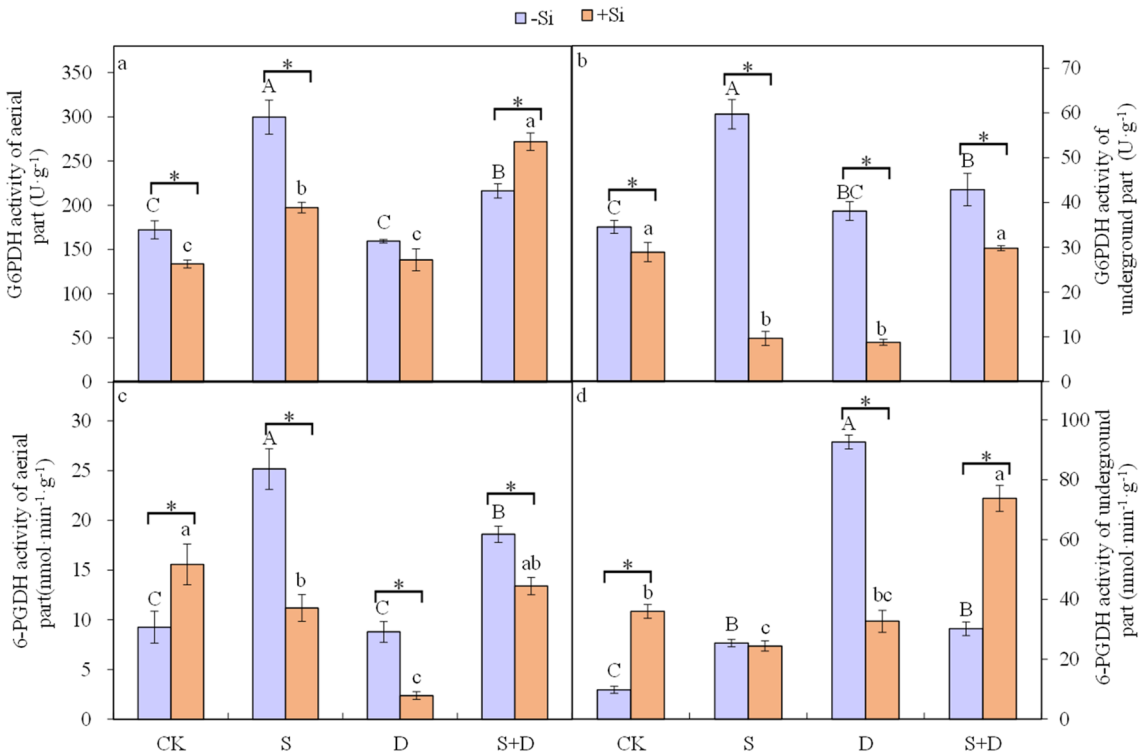


Fig. 7 Effect of exogenous Si on key enzyme activities in PPP in aerial and underground part of *G. uralensis* seedlings grown under different stress. G6PDH, glucose-6-phosphate dehydrogenase; 6-PGDH, 6-phosphogluconic dehydrogenase. The different capital letters indicate the significant difference at $p < 0.05$ within the different treatments without Si, the different lowercase letters indicate the significant difference at $p < 0.05$ within the different treatments with Si addition. The " * " stands for the significant difference at $p < 0.05$ between two treatments under absence of Si and application of Si. Error bars represent the standard error

ICDHm, NAD-MDH, SDH and content of acetyl-CoA to slow down the TCA pathway in the aerial part, which was consistent with the results obtained from the study conducted on cucumber (Li et al. 2020). The reduced acetyl-CoA content might be due to a proportion of acetyl-CoA could be consumed to provide carbon skeletons for increased amino acid synthesis to resist stress (Kazachkova et al. 2013). S stress significantly increased PDH, α-KGDH, SDH and NAD-MDH but decreased ICDH in the underground part. However, GSEA analysis showed

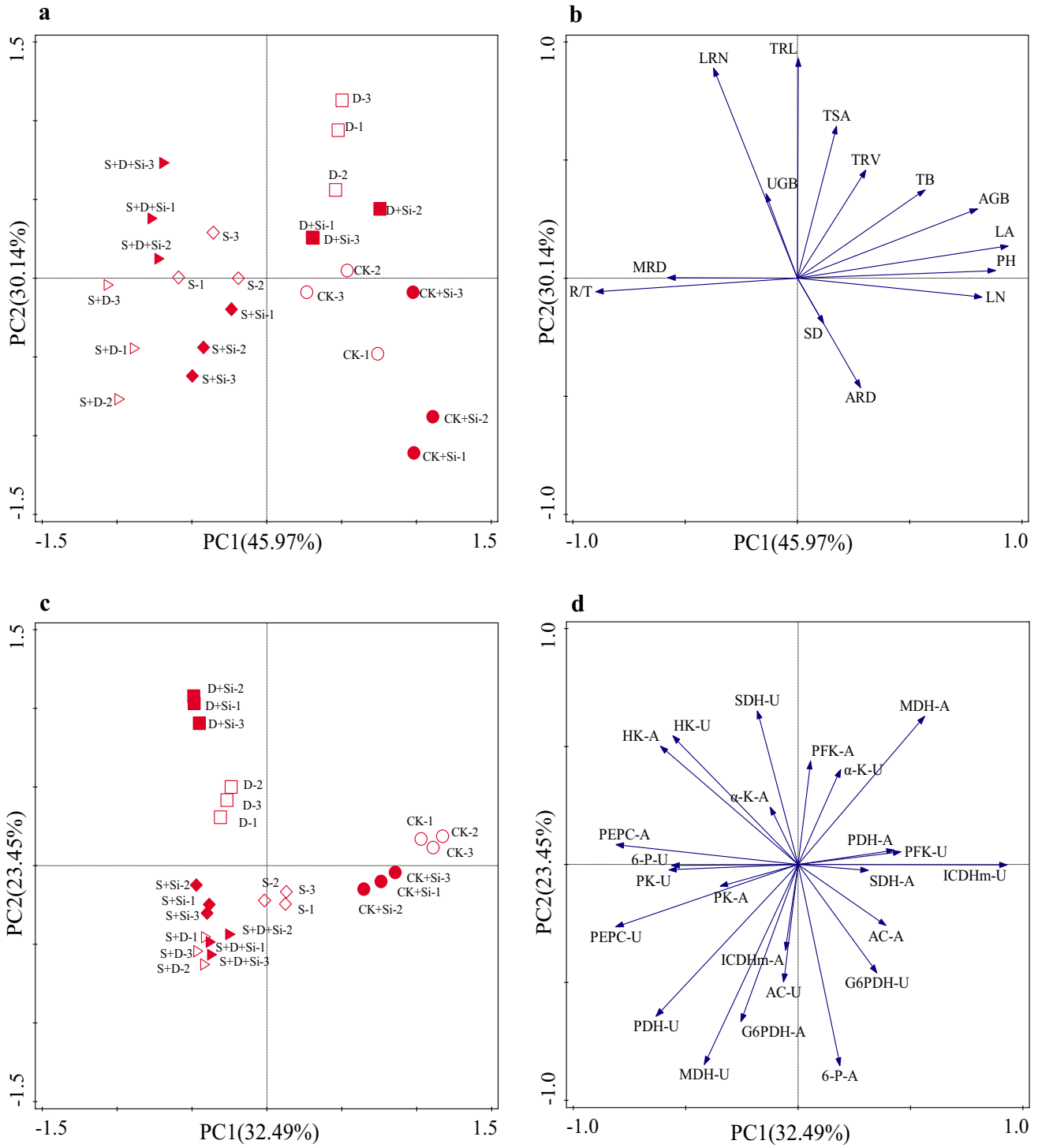
that the TCA pathway was significantly enriched and the whole pathway was downregulated at the transcriptional level in S-U_vs_CK-U comparison (Fig. 9a). Interestingly, PCA results showed that PC1 separated S + Si from S treatment with ICDHm-U being a top contributor (Fig. 8). That was, ICDHm-U may be an important indicator for regulating the TCA cycle in underground part of *G. uralensis* under salt stress. Transcriptome results show that S stress downregulated one gene encoding citrate synthase (CS) in the underground part, possibly reducing the production of energy and citrate by limiting the CS activity, thereby affected the subsequent reaction, which was supported by the results of Xiao et al. (2022). In this case, phosphoenolpyruvate carboxylase (PEPC) activity was enhanced to catalyze PEP to produce OAA in both organs of S-treated plants, thus replenishing intermediates for the TCA cycle, which was consistent with the results of Xiao et al. (2022).

D stress significantly increased α-KGDH and PEPC but decreased PDH, SDH, and NAD-MDH and acetyl-CoA content in aerial part. On the one hand, the increased PEPC could convert a large amount of PEP into OAA, resulting in a lower content of PEP to remain in the EMP pathway, thus decreasing the pyruvate production; on the other hand, D stress induced anaerobic respiration resulting in an increase of pyruvate consumption. Therefore, the TCA cycle was restricted at the substrate level, which further limited the PDH, SDH, and NAD-MDH activities, thus slowing down the TCA process in the aerial part of D-treated plants. However, D stress significantly increased α-KGDH activity, which might be because glutamic acid was regenerated into α-ketoglutaric acid and it entered the TCA cycle, thus stimulating the increased α-KGDH to catalyze α-ketoglutaric acid. This was also reported in *Quercus ilex* seedlings, wherein decreased glutamate levels were observed under drought stress (Rodríguez-Calcerrada et al. 2017). The change in pattern of the underground part in D-stressed plants was basically similar to that of S stress.

The changing trend of related enzymes in the TCA cycle in aerial part under S+D stress resembled that under D stress alone, which inhibited the TCA cycle in general. In addition, combined stress upregulated relative genes encoding PDH, CS, aconitase hydratase and SDH in aerial part, thus slowing down the TCA cycle at the transcriptional level. Combined stresses increased PDH to consume pyruvate caused by increased PK in underground part, producing more acetyl-CoA for TCA cycle. However, S+D stress downregulated one gene encoding CS, which might reduce the citrate synthesis, thereby affecting the subsequent reactions at the substrate level, leading to a decrease of ICDHm and α-KGDH. The GSEA analysis showed that the TCA pathway was significantly enriched and downregulated in S+D-U_vs_CK-U comparison (Fig. 9b), which was consistent with the result at the physiological and biochemical level. In this case, on the one hand, S+D stress might activate the GABA shunt, thereby bypassing the carbon flux from 2-oxoglutarate to succinate via succinyl-CoA. The succinate generated in the GABA shunt could enter the TCA cycle to participate in subsequent reactions, resulting in increase of SDH and NAD-MDH; on the other hand, S+D stress also increased PEPC activity to ensure the normal progress of the TCA cycle.

The GSEA analysis showed that TCA pathway were significantly enriched and upregulated in both aerial and underground parts in S+Si_vs_S comparison (Fig. 9c, d), which suggested that Si addition significantly alleviated the negative effect of salt stress on the TCA metabolism of *G. uralensis* seedlings from the transcriptional level. Si addition significantly decreased PDH and NAD-MDH but increased ICDHm, α-KGDH as well as acetyl-CoA content in the aerial part of S-treated plants. Based on these results, we proposed that, on the one hand, the increase acetyl-CoA might be due to the diversion of acetyl-CoA from secondary metabolites toward the TCA process on account of the mitigation effect of Si on S stress; on the other hand, decreased NAD-MDH result in less OAA reacting with acetyl-CoA, thus finally leading to the accumulation of acetyl-CoA in the aerial part of S-stressed seedlings, which might be responsible for the decrease of PDH because of the feedback inhibition of substrate. Si addition alleviated the inhibitory effect of S stress on ICDHm and increased ICDHm to regulate the C and N metabolism and antioxidant system to cope with salt stress (Xiao et al. 2022), which also led to an increase of α-KGDH to catalyze the extra α-ketoglutarate resulting from increased ICDHm. Si application significantly reduced PDH in the underground part of S-stressed seedlings, probably due to the substrate deficiency caused by Si-induced anaerobic respiration and increased PEPC. This also resulted in subsequent reactions being restricted at the substrate level, consequently declining ICDHm and α-KGDH. However, the increase of PEPC replenished the TCA cycle with amounts of malate, thereby stimulating an increase of NAD-MDH, thus maintaining the function of TCA cycle in the underground part of S-treated plants.

Si addition significantly decreased the SDH in aerial part of D-treated plants, which may contribute to reducing the production of mitochondrial ROS (Jardim-Messederet al. 2015). At the same time, it also resulted in a reduced NAD-MDH substrate, which lead to an insufficient amount of OAA synthesized by NAD-MDH reaction with acetyl CoA. In addition, the decreased PEPC also lead to a reduced replenishment of OAA in the TCA cycle., thus resulting in the accumulation of acetyl COA in aerial part of D-treated plants. Si application significantly decreased α-KGDH and NAD-MDH but increased SDH and PEPC in the underground part of D-stressed plants. This may be because Si



addition activated GABA shunt, which plays a crucial role in preventing the ROS accumulation and regulating nitrogen metabolism (Mahmud et al. 2017; Che-Othman et al. 2020), thereby distributing α-ketoglutarate into GABA shunt and synthesize γ-aminobutyric acid to resist stress (Prabal et al. 2021), resulting in reduced α-KGDH at the substrate level. Subsequently, γ-aminobutyric acid may undergo a series of reactions to convert to succinic acid, which could enter the TCA cycle (Prabal et al. 2021), thus stimulating the SDH activity to catalyze the conversion of succinic acid to fumaric acid. However, Si addition decreased NAD-MDH and thus reduced the synthesis of OAA. As a result, the PEPC is increased to replenish intermediate products for the TCA cycle to ensure its normal progress.

◂**Fig. 8** Principal component analysis of growth parameters and root morphological traits (a and b), enzyme activity in respiration metabolism (c and d) of *G. uralensis* seedlings under eight treatments (CK, CK+Si, S, S+Si, D, D+Si, S+D, S+D+Si). *PH* Plant height, *SD* Stem diameter, *LN* Leaf number, *LA* Leaf area, *AGB* Aboveground biomass, *UGB* Underground biomass, *TB* Total biomass, *TRL* Total root length, *TSA* Total surface aera, *TRV* Total root volume, *MRD* Main root diameter, *ARD* Average root diameter, *LRD* Lateral root number, *HK-A* HK activity in aerial part, *PFK-A* PFK activity in aerial part, *PK-A* PK activity in aerial part, *PDH-A* PDH activity in aerial part, *AC-A* Acetyl-CoA content in aerial part, *ICDHm-A* ICDHm activity in aerial part, *α-K-A* α-KGDH activity in aerial part, *SDH-A* SDH activity in aerial part, *MDH-A* NAD-MDH activity in aerial part, *PEPC-A* PEPC activity in aerial part, *6-P-A* 6-PGDH activity in aerial part, *G6PDH-A* G6PDH activity in aerial part, *HK-U* HK activity in underground part, *PFK-U* PFK activity in underground part, *PK-U* PK activity in underground part, *PDH-U* PDH activity in underground part, *AC-U* Acetyl-CoA content in underground part, *ICDHm-U* ICDHm activity in underground part, *α-K-U* α-KGDH activity in underground part, *SDH-U* SDH activity in underground part, *MDH-U* NAD-MDH activity in underground part, *PEPC-U* PEPC activity in underground part, *6-P-U* 6-PGDH activity in underground part, *G6PDH-U* G6PDH activity in underground part

Si addition significantly alleviated the inhibition effect of S+D stresses on the TCA cycle in the aerial part by increasing PDH, α-KGDH, and NAD-MDH and upregulating three genes encoding CS and α-KGDH in the aerial part of S+D-treated seedlings. Consistently, the EMP and TCA pathway were significantly enriched in both aerial and underground parts, and the overall pathway was upregulated in S+D+Si_vs_S+D comparison (Fig. 9f, h), which indicate that Si addition significantly alleviated the adverse effect of S+D stress on TCA cycle at the transcriptional level. However, Si addition decreased α-KGDH, SDH and content of acetyl-CoA in the underground part of S+D-treated seedlings. This might be because that a portion of acetyl-CoA was used in secondary metabolism to resist stress, thus affecting the subsequent process. In addition, Si addition significantly increased PEPC to replenish TCA cycle intermediates in the underground part of S+D-treated seedlings. Interestingly, PCA results showed that PC1 separated S+D+Si from S+D treatment with PEPC-U being a top contributor (Fig. 8). In other words, PEPC may be an important indicator of the TCA cycle regulation with S+D+Si.

Overall, Si addition alleviated the inhibitory effect of S stress on the TCA cycle by upregulating the TCA pathway at the transcriptional level and regulating acetyl CoA content and related enzyme activities at the physiological and biochemical levels. In addition, Si alleviated the effects of D stress on related enzyme activities and provoked GABA shunt in the underground parts of D-treated plants. Moreover, Si upregulated the TCA pathway at the transcriptional level, inhibited the GABA shunt and increased the PEPC enzyme activity to replenish the TCA cycle with intermediates, and finally alleviated the inhibitory effect of S+D stress on the TCA cycle.

PPP

PPP is another glucose degradation pathway that provides NADPH and substrates for nucleic acid synthesis and the shikimic acid pathway (Sharkey 2021), in which G6PDH and 6PGDH are the two key enzymes. In this study, S stress significantly increased G6PDH and 6-PGDH in both aerial and underground parts. Based on the above results, it was suggested that S stress transformed the EMP–TCA into PPP to enhance salt tolerance in *G. uralensis* seedlings, which has also been observed in salt-tolerant oats (Chen et al. 2021). D stress significantly increased 6-PGDH in the underground part of *G. uralensis* seedlings, which on the one hand promoted PPP and produced more energy to resist D stress, and on the other hand increased 6-PGDH promoted the synthesis of pentose phosphate, a substrate for nucleic acid synthesis, to meet the need for extra lateral roots to absorb more water and relieve stress. Combined stresses significantly increased G6PDH and 6-PGDH and upregulated relative genes in both aerial and underground part to promote PPP, which can provide enough energy for *G. uralensis* seedlings to resist stress.

Si addition decreased G6PDH and 6-PGDH in aerial part, G6PDH enzyme in the underground part, and downregulated two genes encoding FBP and transketolase, respectively, in underground part of S-treated plants to slow down PPP, which may be a symptom of stress relief and mitigation. Si weakened the PPP to avoid excessive carbohydrate consumption, which can probably be attributed to the fact that Si not only mitigated the inhibitory effect of salt stress on the TCA cycle but also accelerated the EMP pathway to provide sufficient energy to resist stress. Similarly, Si addition significantly reduced 6-PGDH in the aerial part and G6PDH and 6-PGDH in the underground part of D-stressed seedlings, indicating that Si significantly relieved D stress and slowed PPP to reduce carbohydrate consumption, resulting in biomass accumulation. However, Si addition increased G6PDH but decreased 6-PGDH in the aerial part, while it was the opposite trend in the underground part of S+D+Si-treated seedlings. In addition, Si addition upregulated a gene encoding 6-phosphogluconolactonase in the aerial part, which could further promote the PPP in S+D-stressed seedlings to provide more energy for resistance to stress.

Overall, Si mitigated the inhibitory effect of stress condition and decelerated PPP in *G. uralensis* seedlings exposed to S or D stress alone and perturbed PPP in those exposed to S+D stress by regulating G6PDH and 6-PGDH activities and related genes, thus providing more energy for subsequent stress- resistant activities in these plants.

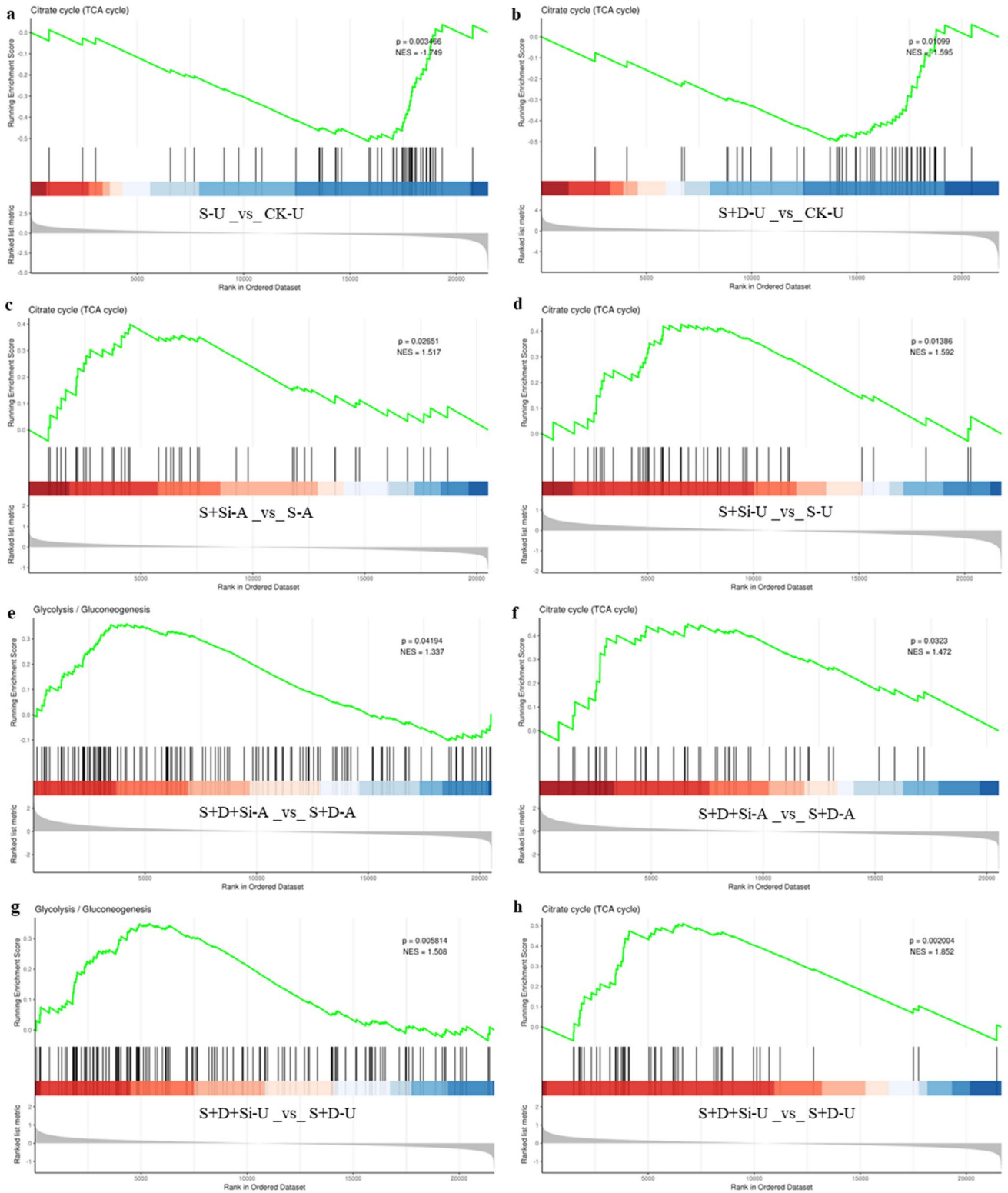


Fig. 9 GSEA analysis of EMP, TCA cycle and PPP pathway in different treatments with $p < 0.05$, FDR < 0.25

Conclusion

Silicon addition effectively mitigated the inhibitory effect of stress on the respiratory metabolism in *G. uralensis* seedlings with different strategies, thus alleviating the inhibitory effect of stress on the growth of *G. uralensis* seedlings to varying degrees. Specifically, under salt stress conditions, Si addition increased leaf number by 15.13%, upregulated the TCA pathway at the transcriptional level, regulated related enzyme activities and increased acetyl CoA content in aerial and underground part by 39.97% and 24.86%, respectively, at the physiological and biochemical levels, thus relieving the inhibitory effect of salt stress on the EMP–TCA process, but weakening PPP by declining G6PDH and 6-PGDH in aerial part by 34.10% and 55.54%, and G6PDH in underground part by 83.86%. Under drought stress, Si application increased underground biomass by 11.40%, slowed the EMP by decreasing PFK in aerial part by 21.76%, PK and PFK in underground part by 38.11% and 64.71%, weakened PPP by reducing 6-PGDH in aerial part by 72.9%, G6PDH and 6-PGDH in underground part by 77.00% and 64.71%. Si increased SDH and PEPC by 28.66% and 145.48% with the TCA cycle and GABA shunt as the main respiratory pathways in the underground part of drought-stressed seedlings. Under combined stresses, Si addition increased leaf number and aboveground biomass by 11.96% and 23.88%, upregulated the EMP and TCA pathways at the transcriptional level, and alleviated the effects of combined stress on EMP–TCA metabolic processes at the physiological and biochemical levels by increasing PDH, α-KGDH and NAD-MDH in aerial part by 27.22%, 18.85% and 140.37%, HK, PK and PEPC in underground part by 93.97%, 25.81% and 31.19%, initiated the replenishment mechanism and inhibited GABA shunt in underground part of *G. uralensis* to provide energy for vital activities.

Funding This work was supported by the National Natural Science Foundation of China (31860343) and the Ningxia Science and Technology Innovation Leader Program (2020GKLRLX12).

Declarations

Competing interests The authors declare no competing interests.

Open Access This article is licensed under a Creative Commons Attribution 4.0 International License, which permits use, sharing, adaptation, distribution and reproduction in any medium or format, as long as you give appropriate credit to the original author(s) and the source, provide a link to the Creative Commons licence, and indicate if changes were made. The images or other third party material in this article are included in the article's Creative Commons licence, unless indicated otherwise in a credit line to the material. If material is not included in the article's Creative Commons licence and your intended use is not permitted by statutory regulation or exceeds the permitted use, you will need to obtain permission directly from the copyright holder. To view a copy of this licence, visit http://creativecommons.org/licenses/by/4.0/.

References

Ahanger MA, Aziz U, Alsahli AA, Alyemeni MN, Ahmad P (2020) Influence of exogenous salicylic acid and nitric oxide on growth, photosynthesis, and ascorbate-glutathione cycle in salt stressed Vigna angularis. Biomolecules 10:42. https://doi.org/10.3390/biom10010042

Ahire ML, Mundada PS, Nikam TD, Bapat VA, Penna S (2021) Multifaceted roles of silicon in mitigating environmental stresses in plants. Plant Physiol Biochem 169:291–310. https://doi.org/10.1016/j.plaphy.2021.11.010

Che-Othman MH, Jacoby RP, Millar AH, Taylor NL (2020) Wheat mitochondrial respiration shifts from the tricarboxylic acid cycle to the GABA shunt under salt stress. New Phytol 225:1047–1048. https://doi.org/10.1111/nph.15713

Chen X, Ding Y, Yang Y, Song C, Wang B, Yang S, Guo Y, Gong Z (2021) Protein kinases in plant responses to drought, salt, and cold stress. J Integr Plant Biol 63:53–78. https://doi.org/10.1111/jipb.13061

Cui JJ, Zhang EH, Zhang XH, Wang Q (2021) Silicon alleviates salinity stress in licorice (*Glycyrrhiza uralensis*) by regulating carbon and nitrogen metabolism. Sci Rep 11:1115. https://doi.org/10.1038/s41598-020-80739-7

Das P, Manna I, Sil P, Bandyopadhyay M, and Biswas. A. K (2021) Silicon augments salt tolerance through modulation of polyamine and GABA metabolism in two indica rice (Oryza sativa L.) cultivars. Plant Physiol Biochem 166:41–52. https://doi.org/10.1016/j.plaphy.2021.05.030

Dhiman P, Rajora N, Bhardwaj S, Sudhakaran SS, Kumar A, Raturi G, Chakraborty K, Gupta OP, Devanna BN, Tripathi DK, Deshmukh R (2021) Fascinating role of silicon to combat salinity stress in plants: an updated overview. Plant Physiol Biochem 162:110–123. https://doi.org/10.1016/j.plaphy.2021.02.023

Du Y, Zhao Q, Chen L, Yao X, Zhang W, Zhang B, Xie F (2020) Effect of drought stress on sugar metabolism in leaves and roots of soybean seedlings. Plant Physiol Biochem 146:1–12. https://doi.org/10.1016/j.plaphy.2019.11.003

Egamberdieva D, Ma H, Alaylar B, Zoghi Z, Kistaubayeva A, Wirth S, Bellingrath-Kimura SD (2021) Biochar amendments improve licorice (*Glycyrrhiza uralensis* Fisch.) Growth and nutrient uptake under salt stress. Plants 10:2135. https://doi.org/10.3390/plants10102135

El-Katony TM, Abdel-Hamid AK, Mergeb SO (2017) Drought stress affects gas exchange and uptake and partitioning of minerals in swallowwort (*Cynanchum acutum* L). Rend Lincei Scienze Fis Naturali 29:23–34. https://doi.org/10.1007/s12210-017-0654-7

ElAtta HA, Aref IM, Ahmed AI (2016) Seed size effects on the response of seedlings of Acacia asak (Forssk.) Willd. to water stress. Pak J Bot 48:439–446

Florea L, Song L, Salzberg SL (2013) Thousands of exon skipping events differentiate among splicing patterns in sixteen human tissues. F1000 Res 2:188. https://doi.org/10.12688/f1000research.2-188.v2

Han YX, Hou ZN, Zhang XM, He QL, Liang ZS (2022) Multi-dimensional "projection"—the impact of abiotic stresses on the content of seven active compounds and expression of related genes in *Glycyrrhiza uralensis* Fisch. Environ Exp Bot 197:104846. https://doi.org/10.1016/j.envexpbot.2022.104846

Hussain S, Shuxian L, Mumtaz M, Shafiq I, Iqbal N, Brestic M, Shoaib M, Sisi Q, Li W, Mei X, Bing C, Zivcak M, Rastogi A, Skalicky M, Hejnak V, Weiguo L, Wenyu Y (2021) Foliar application of

silicon improves stem strength under low light stress by regulating lignin biosynthesis genes in soybean*(Glycine max* (L.) Merr). J Hazard Mater 401:123256. https://doi.org/10.1016/j.jhazmat.2020.123256

Igamberdiev AU, Kleczkowski LA (2021) Pyrophosphate as an alternative energy currency in plants. Biochem J 478(8):1515–1524. https://doi.org/10.1042/BCJ20200940

Jan S, Alyemeni MN, Wijaya L, Alam P, Siddique KH, Ahmad P (2018) Interactive effect of 24-epibrassinolide and silicon alleviates cadmium stress via the modulation of antioxidant defense and glyoxalase systems and macronutrient content in *Pisum sativum* L. seedlings. BMC Plant Biol 18:146. https://doi.org/10.1186/s12870-018-1359-5

Jardim-Messeder D, Caverzan A, Rauber R, Eduardo SF, Margis-Pinheiro M, Galina A (2015) Succinate dehydrogenase (mitochondrial complex II) is a source of reactive oxygen species in plants and regulates development and stress responses. New Phytol 208(3):776–789. https://doi.org/10.1111/nph.13515

Kazachkova Y, Batushansky A, Cisneros A, Tel-Zur N, Fait A, Barak S (2013) Growth platform-dependent and -independent phenotypic and metabolic responses of Arabidopsis and its halophytic relative, Eutrema salsugineum, to salt stress. Plant Physiol 162:1583–1598. https://doi.org/10.1104/pp.113.217844

Li SH, Li YM, Gao Y, He XR, Zhang DL, Liu BB, Li QM (2020) Effects of CO_2 enrichment on non-structural carbohydrate metabolism in leaves of cucumber seedlings under salt stress. Sci Hort. https://doi.org/10.1016/j.scienta.2020.109275

Liao JX, Wang GX (2014) Effects of Drought stress on Leaf Gas Exchange and Chlorophyll fluorescence of *G. uralensis*. Russian J Ecol 45(6):532–538. https://doi.org/10.1134/s1067413614060083

Liu WL, Sun ZR, Qu JX, Yang CN, Zhang XM, Wei XX (2017) Correlation between root respiration and the levels of biomass and glycyrrhizic acid in *G. uralensis*. Exp Ther Med 14:2323–2328. https://doi.org/10.3892/etm.2017.4723

Liu Y, Li P, Xiao L, Wang W, Yu KX, Shi P (2020a) Heterogeneity in short-term allocation of carbon to roots of Pinus tabuliformis seedlings and root respiration under drought stress. Plant Soil 452:359–378. https://doi.org/10.1007/s11104-020-04562-9

Liu Y, Li P, Wang T, Wang W (2020b) Root respiration and belowground carbon allocation respond to drought stress in a perennial grass (*Bothriochloa ischaemum*). Catena. https://doi.org/10.1016/j.catena.2019.104449

Liu JW, Wei Z, Long SJ, Zhao CZ (2021) Maintenance of cell wall integrity under high salinity. Int J Mol Sci 22(6):3260. https://doi.org/10.3390/ijms22063260

Ma Y, Dias MC, Freitas H (2020) Drought and salinity stress responses and microbe-induced tolerance in plants. Front Plant Sci 13:11:591911. https://doi.org/10.3389/fpls.2020.591911

Mahmud JA, Hasanuzzaman M, Nahar K, Rahman A, Hossain MS, Fujita M (2017) γ-gamma-aminobutyric acid (GABA) confers chromium stress tolerance in Brassica juncea L. by modulating the antioxidant defense and glyoxalase systems. Ecotoxicology 26:675–690. https://doi.org/10.1007/s10646-017-1800-9

Malik MA, Wani AH, Mir SH, Rehman IU, Tahir I, Ahmad P, Rashid I (2021) Elucidating the role of silicon in drought stress tolerance in plants. Plant Physiol Biochem 165:187–195. https://doi.org/10.1016/j.plaphy.2021.04.021

Mundada PS, Barvkar VT, Umdale SD, Kumar A, Nikam S, T. D., and Ahire ML, (2021) An insight into the role of silicon on retaliation to osmotic stress in finger millet *(Eleusine coracana* (L.) Gaertn). J Hazard MaterDoi. https://doi.org/10.1016/j.jhazmat.2020.124078

Poór P, Gémes K, Horváth F, Szepesi Á, Simon ML, Tari I (2011) Salicylic acid treatment via the rooting medium interferes with stomatal response, CO_2 fixation rate and carbohydrate metabolism in tomato, and decreases harmful effects of subsequent salt stress. Plant Biol 13(1):105–114. https://doi.org/10.1111/j.1438-8677.2010.00344.x

Poór P, Patyi G, Takács Z, Szekeres A, Tari I (2019) Salicylic acid-induced ROS production by mitochondrial electron transport chain depends on the activity of mitochondrial hexokinases in tomato *(Solanum lycopersicum* L.). J Plant Res 132:273–283. https://doi.org/10.1007/s10265-019-01085-y

Prabal D, Indrani M, Palin S, Maumita B, Asok KB (2021) Silicon augments salt tolerance through modulation of polyamine and GABA metabolism in two indica rice (Oryza sativa L.) cultivars. Plant Physiol Biochem 166:41–52. https://doi.org/10.1016/j.plaphy.2021.05.030

Rodríguez-Calcerrada J, Rodrigues AM, Perdiguero P, António C, Atkin OK, Li M, Collada C, Gil L (2017) A molecular approach to drought-induced reduction in leaf CO_2 exchange in drought-resistant *Quercus ilex*. Physiol Plant 162(4):394–408. https://doi.org/10.1111/ppl.12649

Sharkey TD (2021) Pentose phosphate pathway reactions in photosynthesizing cells. Cells 10:1547. https://doi.org/10.3390/cells10061547

Shen Zh, Cheng XJ, Li X, Deng XY, Dong XX, Wang SM, Pu XZ (2022) Effects of silicon application on leaf structure and physiological characteristics of *Glycyrrhiza uralensis* Fisch. and *Glycyrrhiza infata* Bat.under salt treatment. BMC Plant Biol 22:390. https://doi.org/10.1186/s12870-022-03783-7

Sui N, Wang Y, Liu SS, Yang Z, Wang F, Wan SB (2018) Transcriptomic and physiological evidence for the relationship between unsaturated fatty acid and salt stress in peanut. Front Plant Sci 9:7. https://doi.org/10.3389/fpls.2018.00007

Tagnon MD, Simeon KO (2017) Aldehyde dehydrogenases may modulate signaling by lipid peroxidation-derived bioactive aldehydes. Plant Signal Behav. https://doi.org/10.1080/15592324.2017.1387707

Tang J, Bassham DC (2021) Autophagy during drought: function, regulation, and potential application. Plant J. https://doi.org/10.1111/tpj.15481

Verbeke S, Padilla-Díaz CM, Martínez-Arias C, Goossens W, Haesaert G, Steppe K (2023) Mechanistic modeling reveals the importance of turgor-driven apoplastic water transport in wheat stem parenchyma during carbohydrate mobilization. New Phytol 237(2):423–440. https://doi.org/10.1111/nph.18547

Verma KK, Song XP, Zeng Y, Li DM, Guo DJ, Rajput VD, Chen GL, Barakhov A, Minkina TM, Li YR (2020) Characteristics of leaf stomata and their relationship with photosynthesis in *Saccharum officinarum* under drought and silicon application. ACS Omega 5:24145–24153. https://doi.org/10.1021/acsomega.0c03820

Weiszmann J, Fürtauer L, Weckwerth W, Nägele T (2018) Vacuolar sucrose cleavage prevents limitation of cytosolic carbohydrate metabolism and stabilizes photosynthesis under abiotic stress. FEBS J 21(285):4082–4098. https://doi.org/10.1111/febs.14656

Wu J, Wang J, Hui W, Zhao F, Wang P, Su C, Gong W (2022) Physiology of plant responses to water stress and related genes: a review. Forests 13:324. https://doi.org/10.3390/f13020324

Xiao X, Wang Q, Ma X, Lang DY, Guo Z, Zhang XH (2022) Physiological biochemistry-combined transcriptomic analysis reveals mechanism of *Bacillus cereus* G2 improved salt-stress tolerance of *Glycyrrhiza uralensis* Fisch. seedlings by balancing carbohydrate metabolism. Front Plant Sci 12:712363. https://doi.org/10.3389/fpls.2021.712363

Xie ZC, Chu YK, Zhang WJ, Lang DY, Zhang XH (2019) *Bacillus pumilus* alleviates drought stress and increases metabolite accumulation in *Glycyrrhiza uralensis* Fisch. Environ Exp Bot 158:99–106. https://doi.org/10.1016/j.envexpbot.2018.11.021

Xu Y (2022) Fu XY (2022) Reprogramming of plant central metabolism in response to abiotic stresses: a metabolomics view. Int J Mol Sci 23:5716. https://doi.org/10.3390/ijms23105716

Yao H, Wang F, Bi Q, Liu H, Liu L, Xiao G, Zhu J, Shen H, Li H (2022) Combined analysis of pharmaceutical active ingredients and transcriptomes of *Glycyrrhiza uralensis* under PEG6000-induced drought stress revealed glycyrrhizic acid and flavonoids accumulation via JA-mediated signaling. Front Plant Sci 13:920172. https://doi.org/10.3389/fpls.2022.920172

Zhang WJ, Xie ZC, Wang L, Li M, Lang DY, Zhang XH (2017) Silicon alleviates salt and drought stress of *Glycyrrhiza uralensis* seedling by altering antioxidant metabolism and osmotic adjustment. J Plant Res 130:611–624. https://doi.org/10.1007/s10265-017-0927-3

Zhang WJ, Yu XX, Li M, Lang DY, Zhang XH, Xie ZC (2018) Silicon promotes growth and root yield of *Glycyrrhiza uralensis* under salt and drought stresses through enhancing osmotic adjustment and regulating antioxidant metabolism. Crop Prot 107:1–11. https://doi.org/10.1016/j.cropro.2018.01.005

Zhang WJ, Zhang XJ, Lang DY, Li M, Liu H, Zhang XH (2020) Silicon alleviates salt and drought stress of *Glycyrrhiza uralensis* plants by improving photosynthesis and water status. Biol Plant 64:302–313. https://doi.org/10.32615/bp.2019.136

Zhang GF, Zhou JZ, Peng Y, Tan ZD, Li L, Yu LQ, Jin C, Fang S, Lu SP, Guo L, Yao X (2022) Genome-wide association studies of salt tolerance at seed germination and seedling stages in *Brassica napus*. Front Plant Sci 12:772708. https://doi.org/10.3389/fpls.2021.772708

Zhong M, Yuan YH, Shu S, Sun J, Guo S, Yuan R, Tang YY (2016) Effects of exogenous putrescine on glycolysis and Krebs cycle metabolism in cucumber leaves subjected to salt stress. Plant Growth Regul 79(3):319–330. https://doi.org/10.1007/s10725-015-0136-9

Zhong C, Chen C, Gao X, Tan C, Bai H, Ning K (2022) Multi-omics profiling reveals comprehensive microbe-plant-metaboliteregulation patterns for medicinal plant *Glycyrrhiza uralensis* Fisch. Plant Biotechnol. https://doi.org/10.1111/pbi.1386

Zhou CP, Bai T, Wang Y, Wu T, Zhang XZ, Xu XF, Han ZH (2017) Morpholoical and enzymatic responses to waterlogging in three *Prunus* species. Sci Hort 221:62–67. https://doi.org/10.1016/j.scienta.2017.03.054

Zhou J, Chen SQ, Shi WJ, Rakefet D, Li ST, Yang FL, Lin ZX (2021) Transcriptome profiling reveals the effects of drought tolerance in Giant Juncao. BMC Plant Biol 21:2. https://doi.org/10.1186/s12870-020-02785-7

Publisher's Note Springer Nature remains neutral with regard to jurisdictional claims in published maps and institutional affiliations.